Hadronic Calorimeters

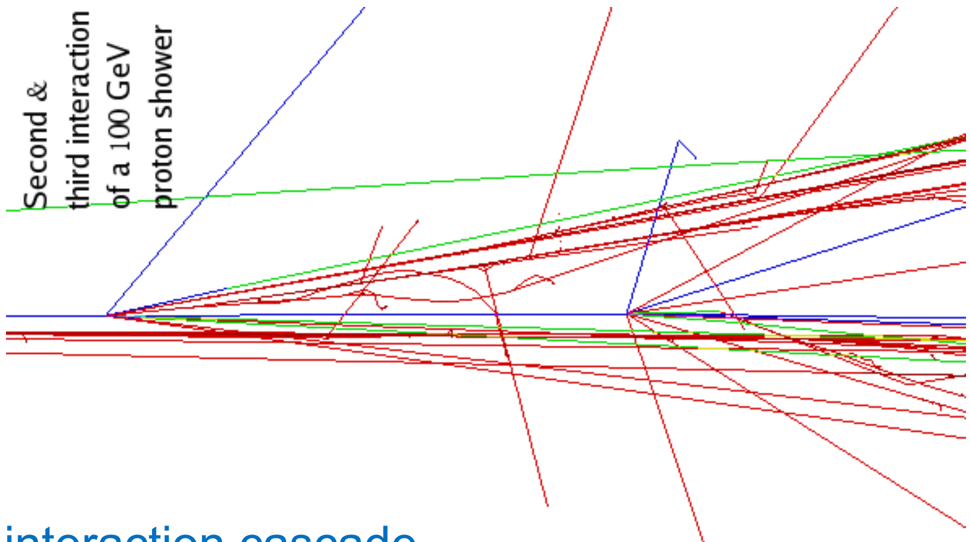

- Strong (nuclear) interaction cascade
- Similar to EM shower

$$\chi_0(EM) \rightarrow \lambda_I(had) \approx 35\, g\, cm^{-2}\, A^{1/3}$$

hadronic interaction length

$$\lambda_I > \chi_0$$

hadronic calorimeter
nearly always sampling calorimeters

- Shower length $\sim 5\lambda \sim 4m @ 100\, GeV$
  $\sim 13\lambda \sim 10m @ 1\, TeV$

- Energy Resolution
  - shower fluctuations
  - leakage of energy
  - invisible energy loss mechanisms

Sampling Calorimeter

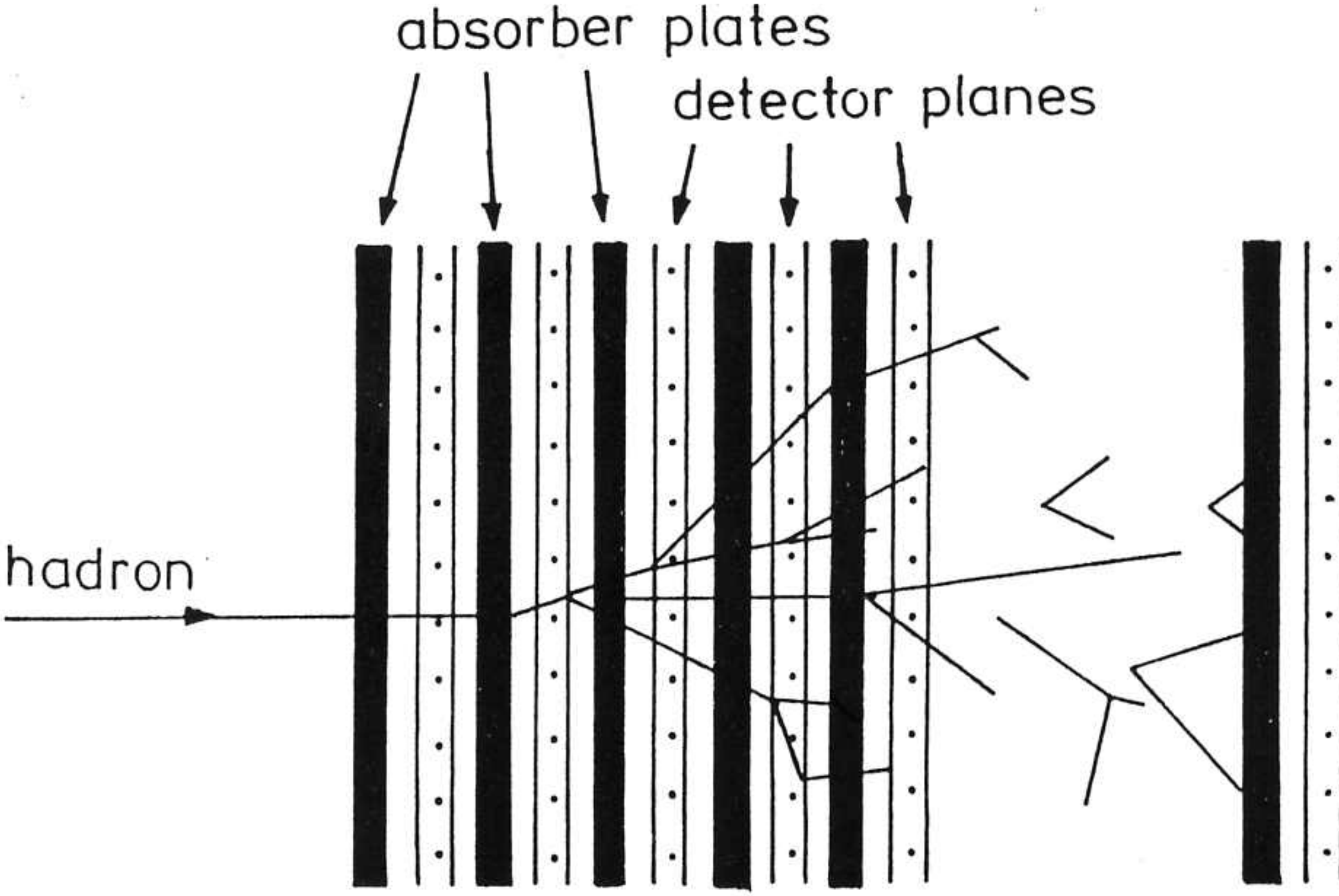

Hadronic Lateral Shower Profile

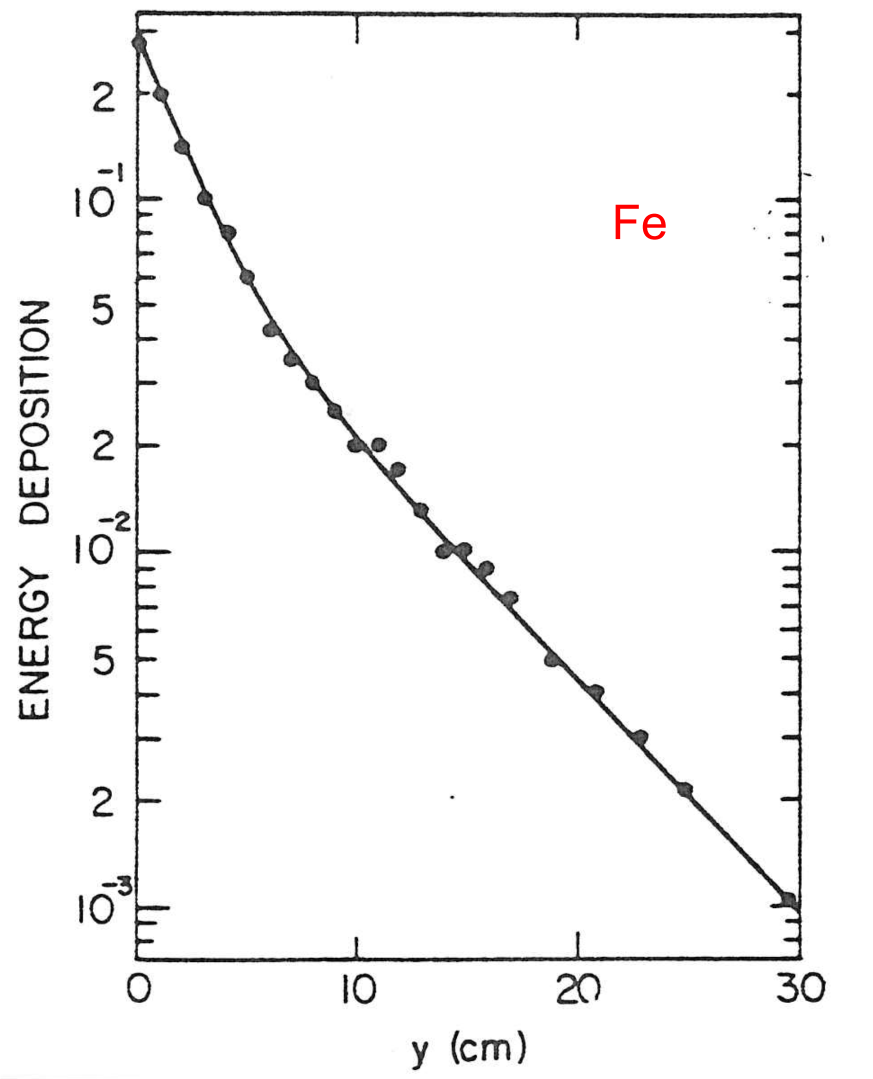

- Hadronic shower much broader than EM
  - Mean hadronic p_T versus MCS

Fe λ_I : $16\,cm$

χ_0 : $1.8\,cm$

Hadronic Shower Longitudinal Development

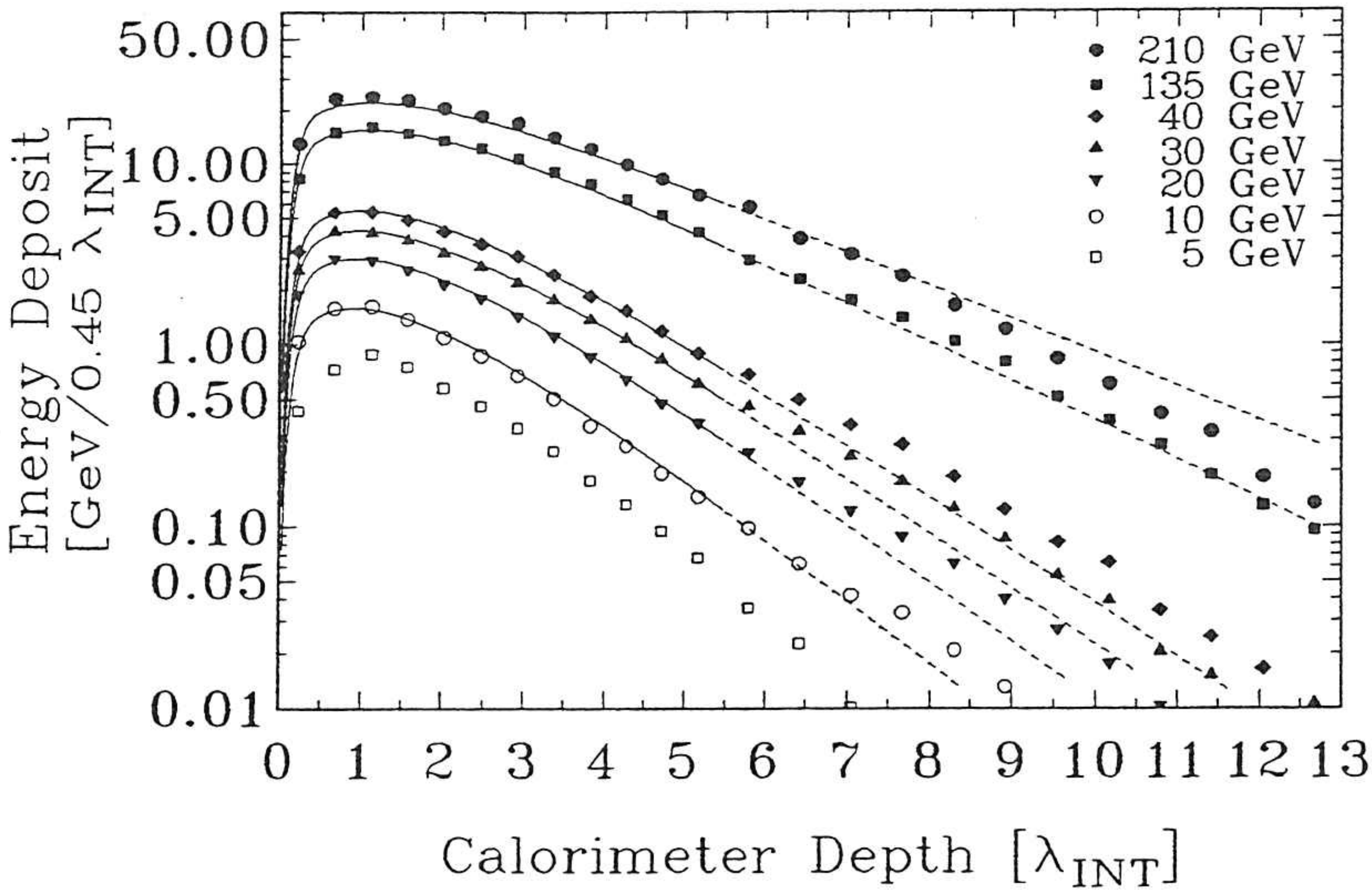

ZEUS
Uranium/Scint

Lateral Scaling with Material

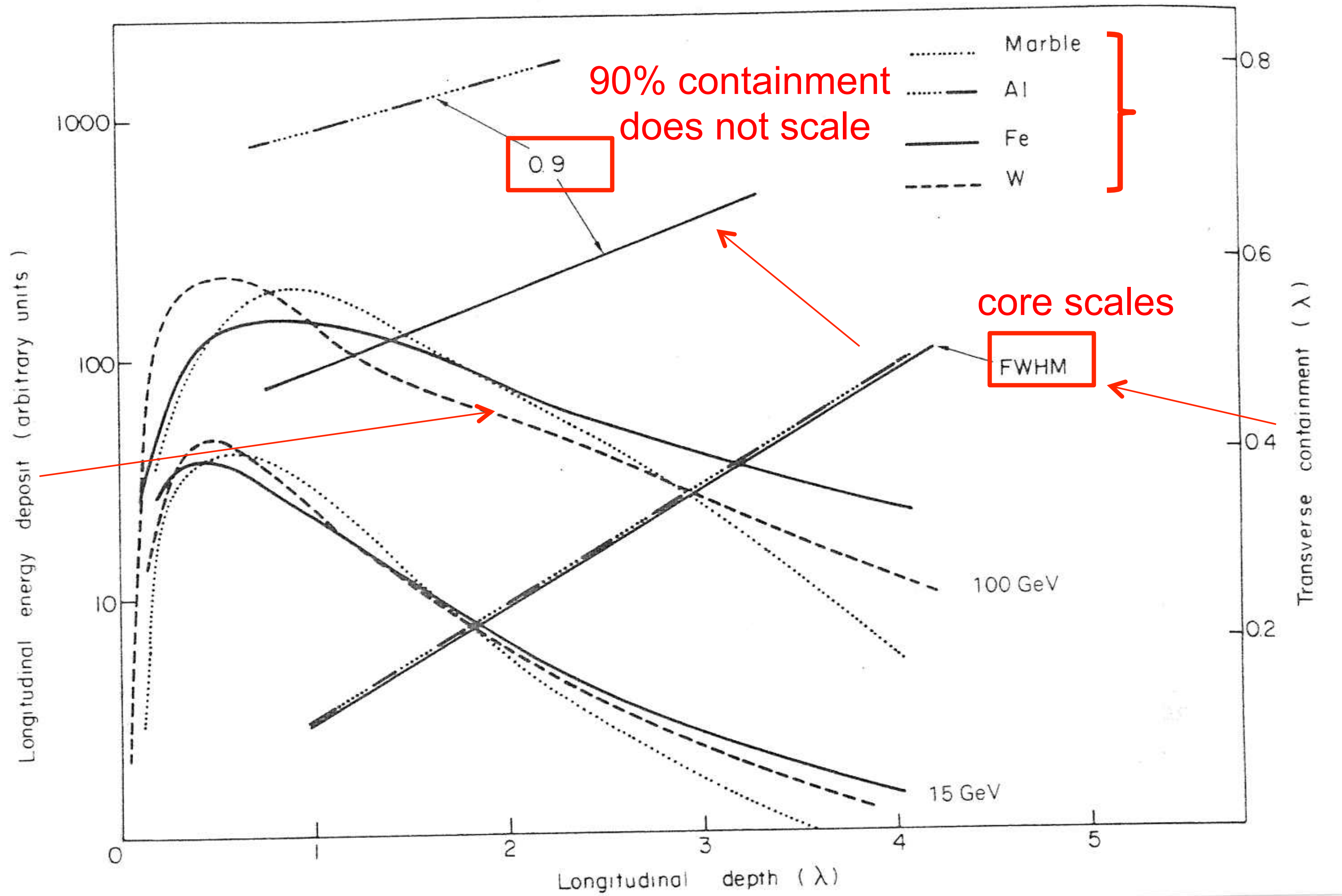

Calorimeter Energy Resolution

$$\left(\frac{\sigma}{E}\right)^2 = \left(\frac{A_0}{\sqrt{E}}\right)^2 + \left(\frac{A_1}{\sqrt{E}}\right)^2 + (A_2 \ln E)^2 + \left(\frac{A_3\sqrt{N}}{E}\right)^2 + A_4$$

$\frac{A_0}{\sqrt{E}}$ sampling and shower fluctuations

number of samples $N = \frac{E}{\Delta E}$ ← energy (E); ← energy deposited in a sampling step (ΔE)

$$\sigma_E = \sigma_N \cdot \Delta E = \sqrt{N} \cdot \Delta E$$

$$\frac{\sigma_E}{E} = \sqrt{N}\frac{\Delta E}{E}$$

$$\frac{\sigma_E}{E} = \frac{\sqrt{\Delta E}}{\sqrt{E}}$$

stochastic term $A_0 \sim \sqrt{\Delta E}$

Calorimeter Energy Resolution

$$\left(\frac{\sigma}{E}\right)^2 = \left(\frac{A_0}{\sqrt{E}}\right)^2 + \left(\frac{A_1}{\sqrt{E}}\right)^2 + (A_2 \ln E)^2 + \left(\frac{A_3\sqrt{N}}{E}\right)^2 + A_4$$

$\frac{A_1}{\sqrt{E}}$ counting statics in sensor system

e.g. # of photo-electrons in PM, ion pairs in liquid argon

$$N = \bar{n} \cdot E$$

mean # of photo-electrons in PM per unit of incident energy

$$\sigma_E = \frac{\sigma_N}{\bar{n}} = \frac{\sqrt{N}}{\bar{n}} = \frac{\sqrt{\bar{n} \cdot E}}{\bar{n}}$$

$$\frac{\sigma_E}{E} = \frac{1}{\sqrt{\bar{n}}} \cdot \frac{1}{\sqrt{E}} \qquad A_1 = \frac{1}{\sqrt{\bar{n}}}$$

this term is usually negligible

A_2 shower leakage fluctuations – make calorimeter as deep as $$ allow

Calorimeter Energy Resolution

$$\left(\frac{\sigma}{E}\right)^2 = \left(\frac{A_0}{\sqrt{E}}\right)^2 + \left(\frac{A_1}{\sqrt{E}}\right)^2 + \left(A_2 \ln E\right)^2 + \left(\frac{A_3\sqrt{N}}{E}\right)^2 + A_4$$

A_3 noise - detector or electronics
- important for low level signal
- liquid argon electronics
- detector capacitance

N channels with some intrinsic noise $\Sigma \rightarrow N \cdot \Delta E$ ← noise (energy)

$$\frac{\sigma_E}{E} = N\frac{\Delta E}{E}$$

← deposited energy

$\frac{1}{E}$ behaviour

A_3 ; $\Delta E \cdot N$ increases with number of channels summed over

Calorimeter Energy Resolution

$$\left(\frac{\sigma}{E}\right)^2 = \left(\frac{A_0}{\sqrt{E}}\right)^2 + \left(\frac{A_1}{\sqrt{E}}\right)^2 + (A_2 \ln E)^2 + \left(\frac{A_3\sqrt{N}}{E}\right)^2 + A_4$$

A_4 inter - calibration uncertainty of channels - constant in E

- fractional channel to channel gain uncertainty
- spatial in-homogeneity of detector energy response
- dead space
- temperature variation
- radiation damage
- all these influence spatial variation of effective energy response

$$\sigma = k \cdot E$$

$$\frac{\sigma_E}{E} = k$$ constant

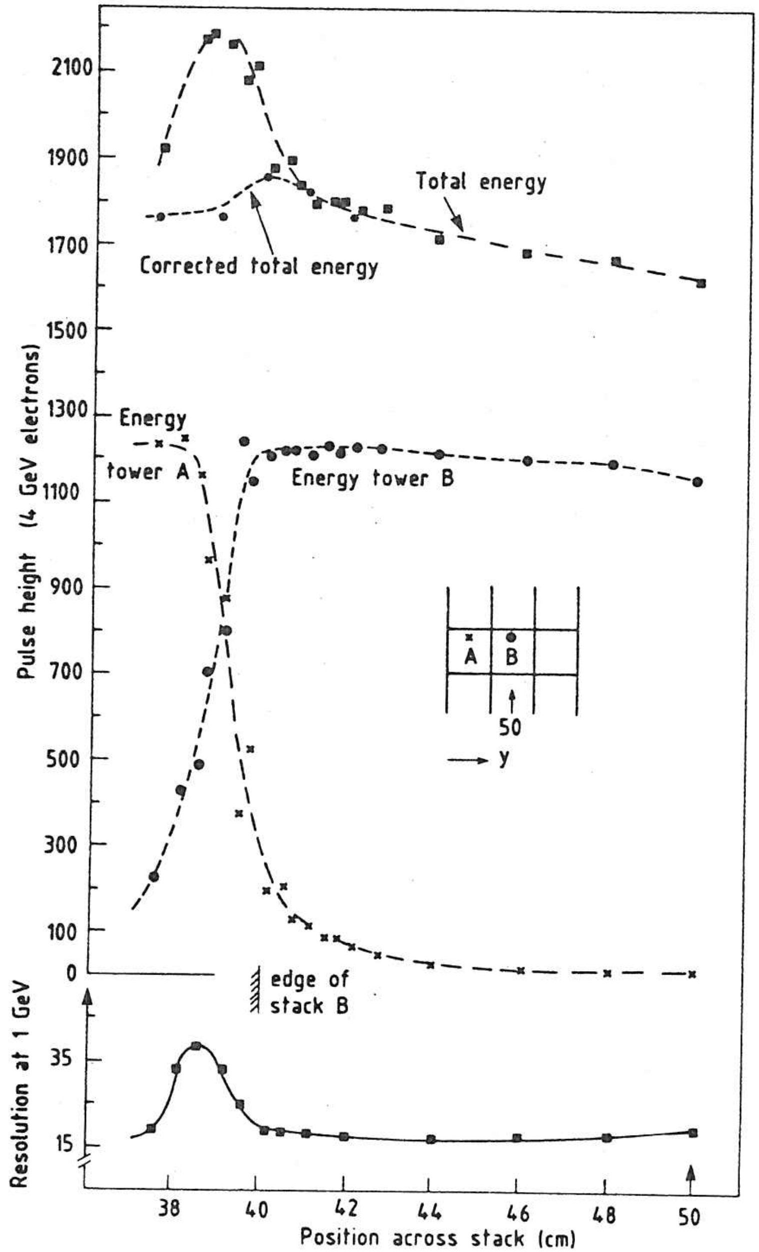

Calorimeter non-uniformity

Table 5: Principal Contributions to Energy Resolution in Electromagnetic and Hadronic Calorimeters

<table>
<tr><th>Mechanisms
(add in quadrature)</th><th>Electromagnetic showers</th><th>Hadronic showers</th></tr>
<tr><td>Intrinsic shower fluctuations</td><td>Track-length fluctuations:
$\sigma/E \gtrsim 0.005/\sqrt{E}$ (GeV).</td><td>Fluctuations in the energy loss:
$\sigma/E \simeq 0.45/\sqrt{E}$ (GeV).
Scaling weaker than $1/\sqrt{E}$ for high energies. With compensation for nuclea effects: $\sigma/E \simeq 0.22/\sqrt{E}$ (GeV).</td></tr>
<tr><td>Sampling fluctuations</td><td>$\sigma/E \simeq 0.04\sqrt{\Delta E/E}$.
Nature of readout may augment sampling fluctuations.</td><td>$\sigma/E \simeq 0.09\sqrt{\Delta E/E}$</td></tr>
<tr><td>Instrumental effects</td><td colspan="2">Noise and pedestal width: $\sigma/E \sim 1/E$
– determine minimum detectable signal;
– limit low-energy performance.

Calibration errors and non-uniformities:
$\sigma/E \sim$ constant and therefore limits high-energy performance.</td></tr>
<tr><td>Incomplete containment of shower</td><td colspan="2">$\sigma/E \sim E^{-\alpha}$, $\alpha < 1/2$
(see subsec. 2.2, resp. 3.4).
For leakage fraction $\geq$ few %:
non-linear response and non-Gaussian ‘tail’.</td></tr>
</table>

Semi-empirical model of hadron shower development

$$\frac{dE}{dS} = E_{INC}\left\{\frac{Cx^{(\alpha_E-1)}e^{-x}}{\Gamma(\alpha_E)}\right\} + E_{INC}(1-C)\left\{\frac{y^{(\alpha_H-1)}e^{-y}}{\Gamma(\alpha_H)}\right\}$$

electromagnetic part

hadronic part

$$x \equiv \beta_E \frac{(S-S_0)}{\chi_0}$$

radiation length

$$y \equiv \beta_H \frac{(S-S_0)}{\lambda}$$

interaction length

$$\alpha_H = \alpha_E = 0.62 + 0.32 \ln E$$
$$\beta_H = 0.91 - 0.02 \ln E$$
$$\beta_E = 0.22$$
$$C = 0.46$$

$S_0 \neq 0$ - significant amount of material in front of calorimeter (magnet coil etc.)

More Rules of Thumb for the Hobbyist

- Shower maximum

$$t_{\max}(\lambda) \sim 0.2 \ln E(GeV) + 0.7$$

- 95% Longitudinal containment

$$L_{95\%}(\lambda) \sim t_{\max} + 2.5\lambda_{ATT}$$

$$\lambda_{ATT} \approx \lambda\left[E(GeV)\right]^{0.13}$$

- 95% Lateral containment

$$R_{95\%} \sim 1\lambda$$

- Mixtures in sampling calorimeters

active + passive material

$$\frac{1}{\chi_{eff}} = \sum_i \frac{f_i}{\chi_0^i}$$

FRACTION BY WEIGHT.

$$f_{act} = \frac{m_{act}}{m_{act} + m_{pass}}$$

$$\frac{\varepsilon_{eff}^{crit}}{\chi_{eff}} = \sum_i f_i \frac{\varepsilon_i^{crit}}{\chi_0^i}$$

$$\frac{E_{vis}}{E_{inc}} = f_{act} \frac{\varepsilon_{act}^{crit} / \chi_0^{act}}{\varepsilon_{eff}^{crit} / \chi_{eff}}$$

Typical Calorimeter Resolutions

- Homogeneous EM (crystal, glass)

$$\frac{0.5\%}{\sqrt{E}} \rightarrow \frac{3.0\%}{\sqrt{E}} \oplus 0.5\%$$

CLEO, Crystal Ball, Belle, CMS.....

- Sampling EM (Pb/Scint, Pb/LAr)

$$\frac{8\%}{\sqrt{E}} \rightarrow \frac{15\%}{\sqrt{E}} \oplus 1\%$$

CDF, ZEUS, ALEPH, ATLAS.....

- Non-compensating HAD (Fe/Scint, Fe/LAr)

$$\frac{70\%}{\sqrt{E}} \rightarrow \frac{110\%}{\sqrt{E}} \oplus 5\%$$

CDF,ATLAS,H1, LEP = everyone

  - Compensating HAD (DU/Scint)

$$\frac{35\%}{\sqrt{E}} \oplus 1\%$$

ZEUS, HELIOS

Invisible Energy in Hadronic Showers

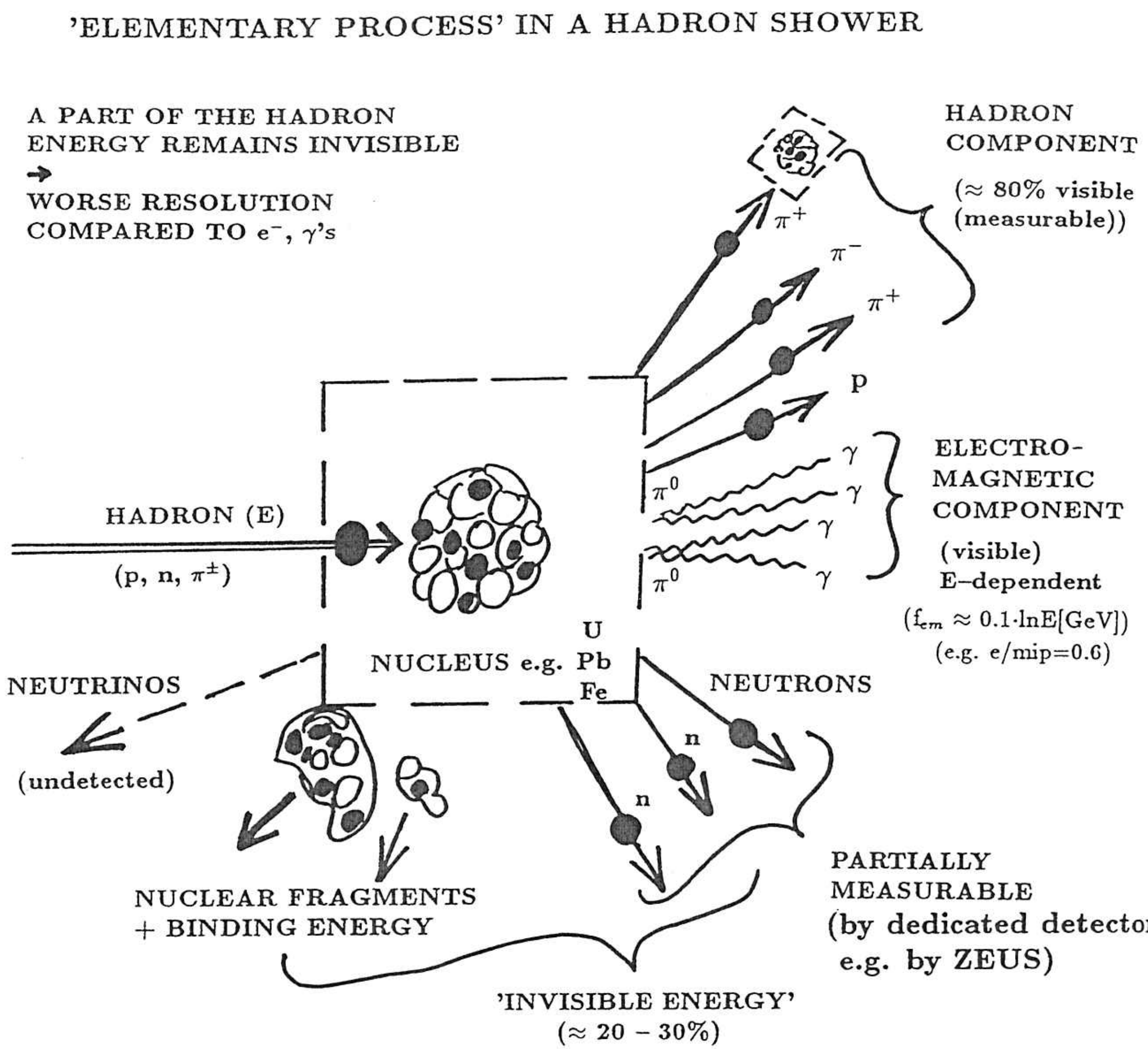

Fig. 3.6 'Elementary physical process' in a hadron shower.

Difference in Response to Electrons and Hadrons

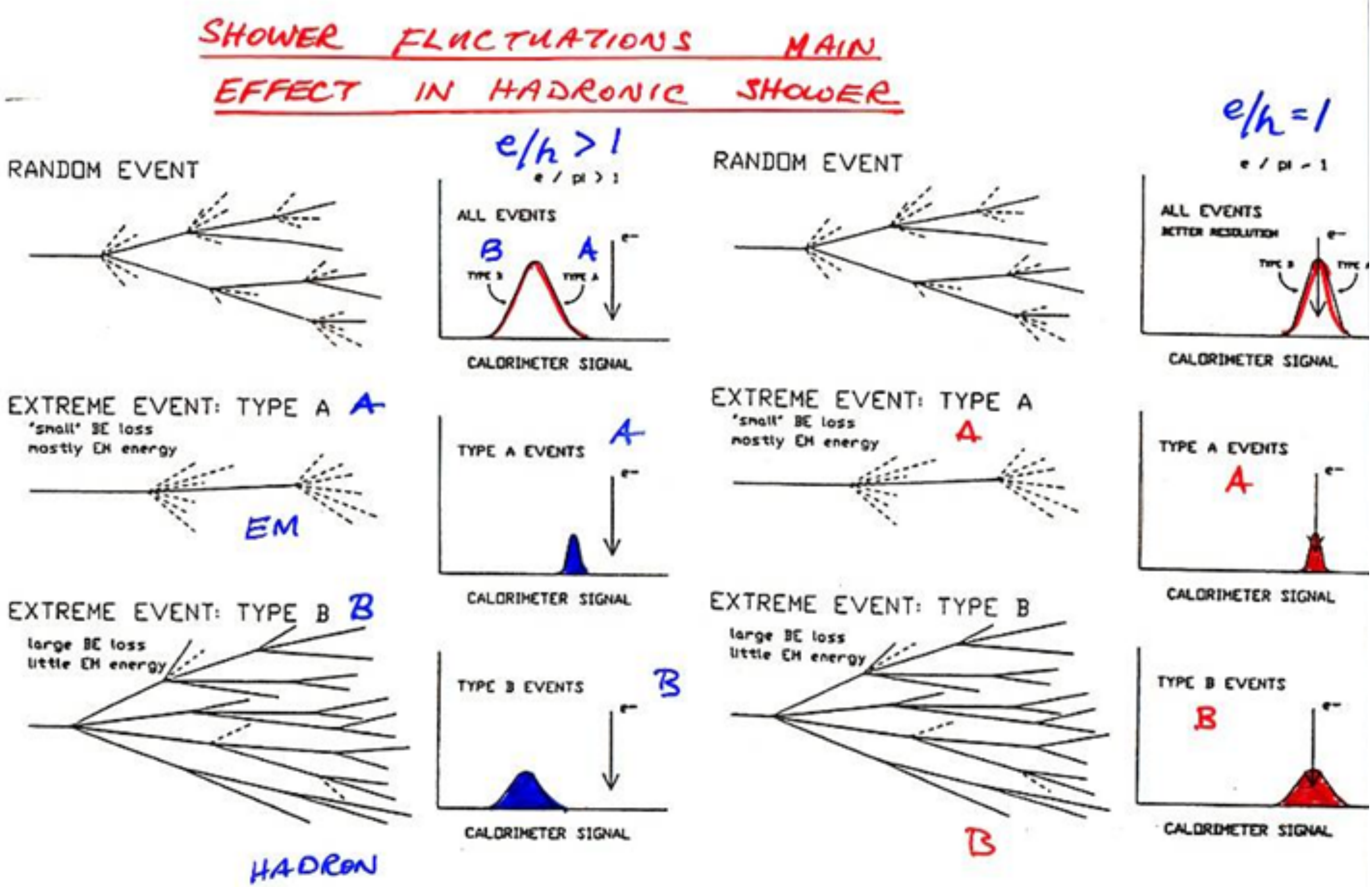

Effect of e/h on Energy Resolution

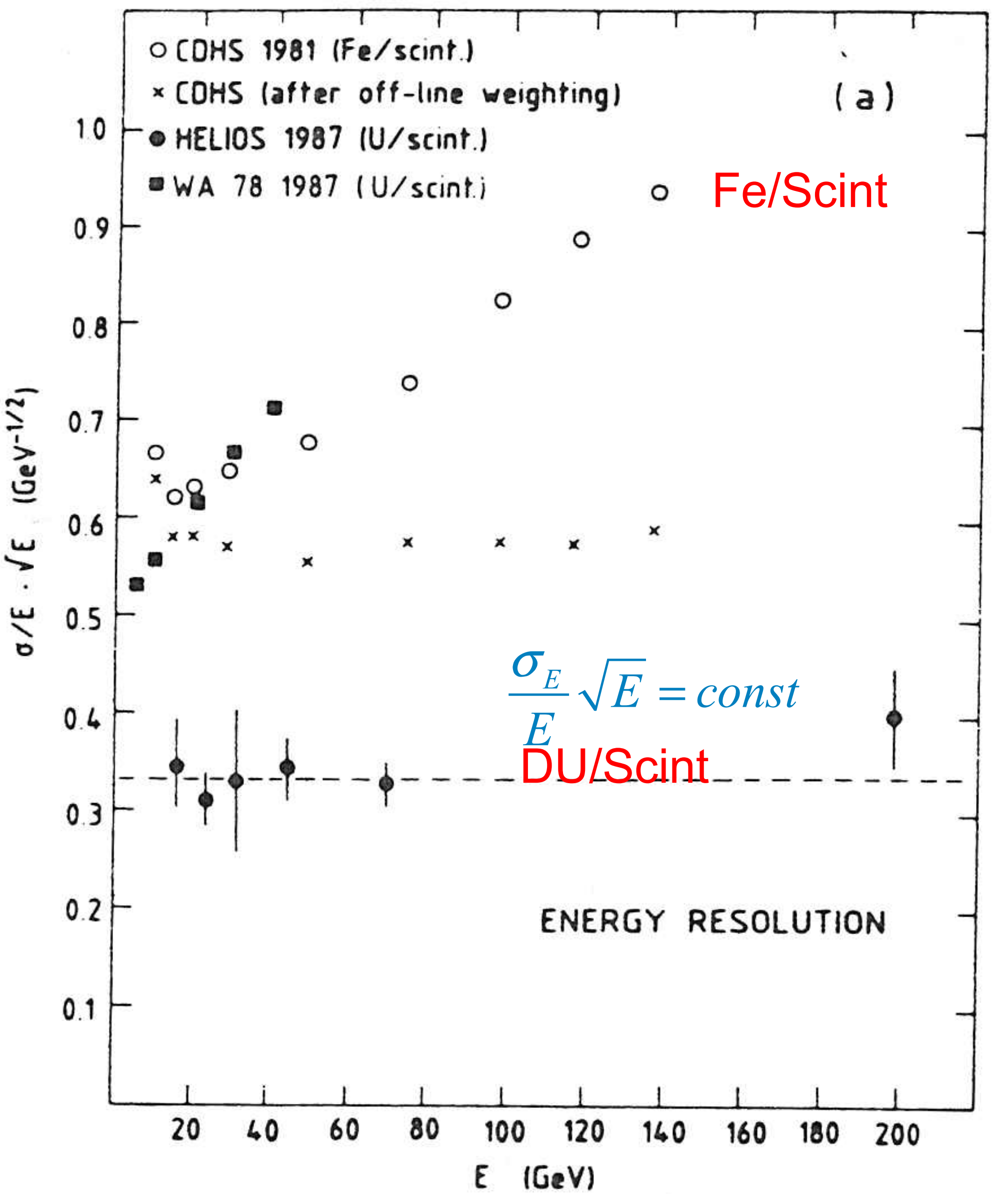

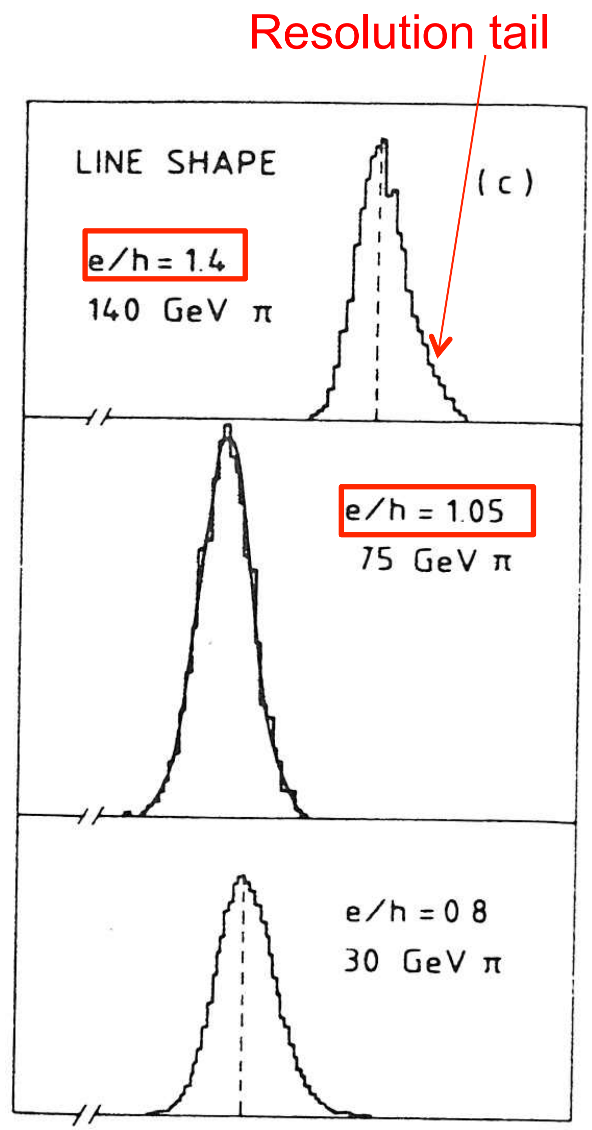

Effect of e/h on Linearity

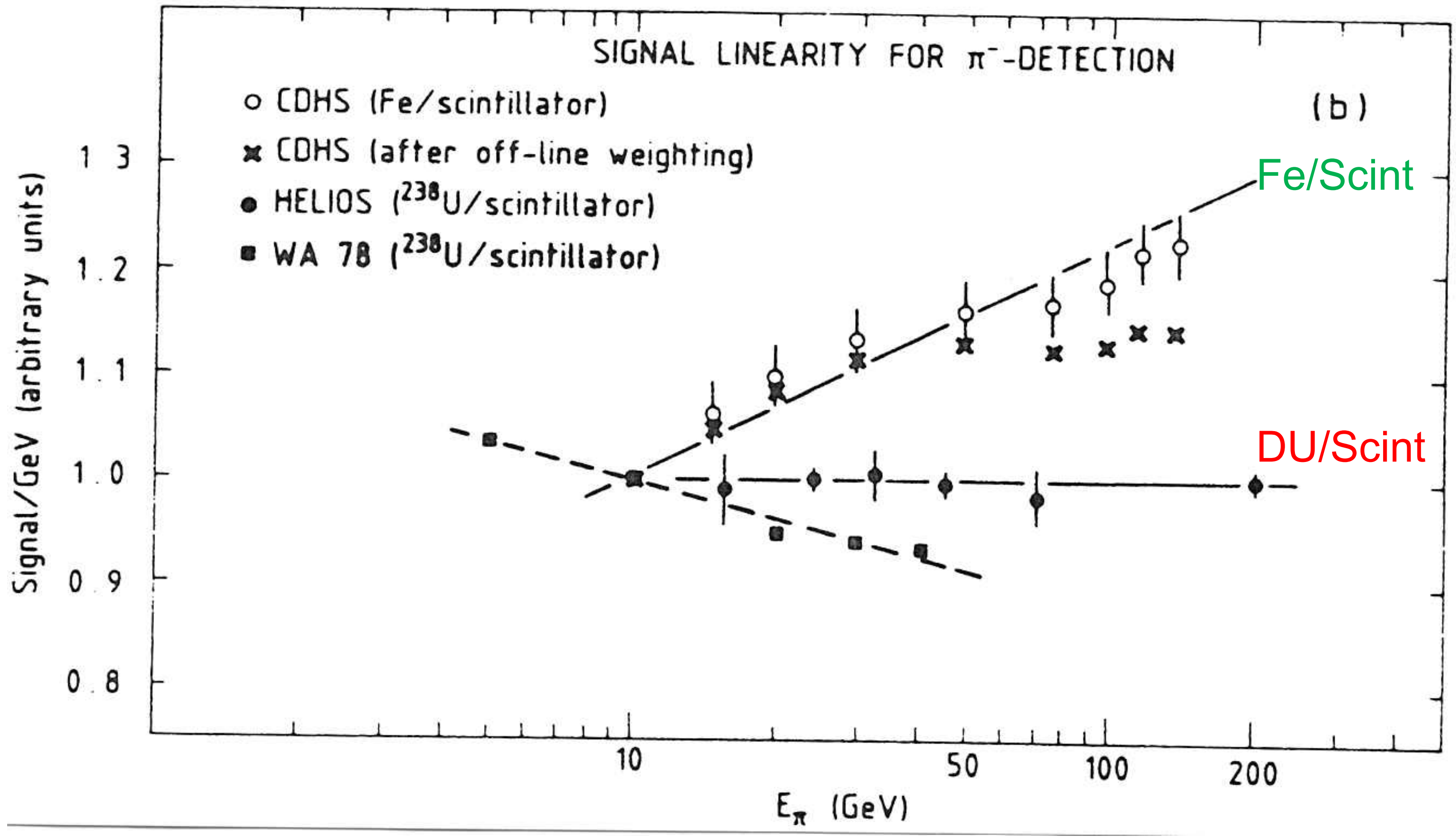

Physics of Sampling Calorimetry

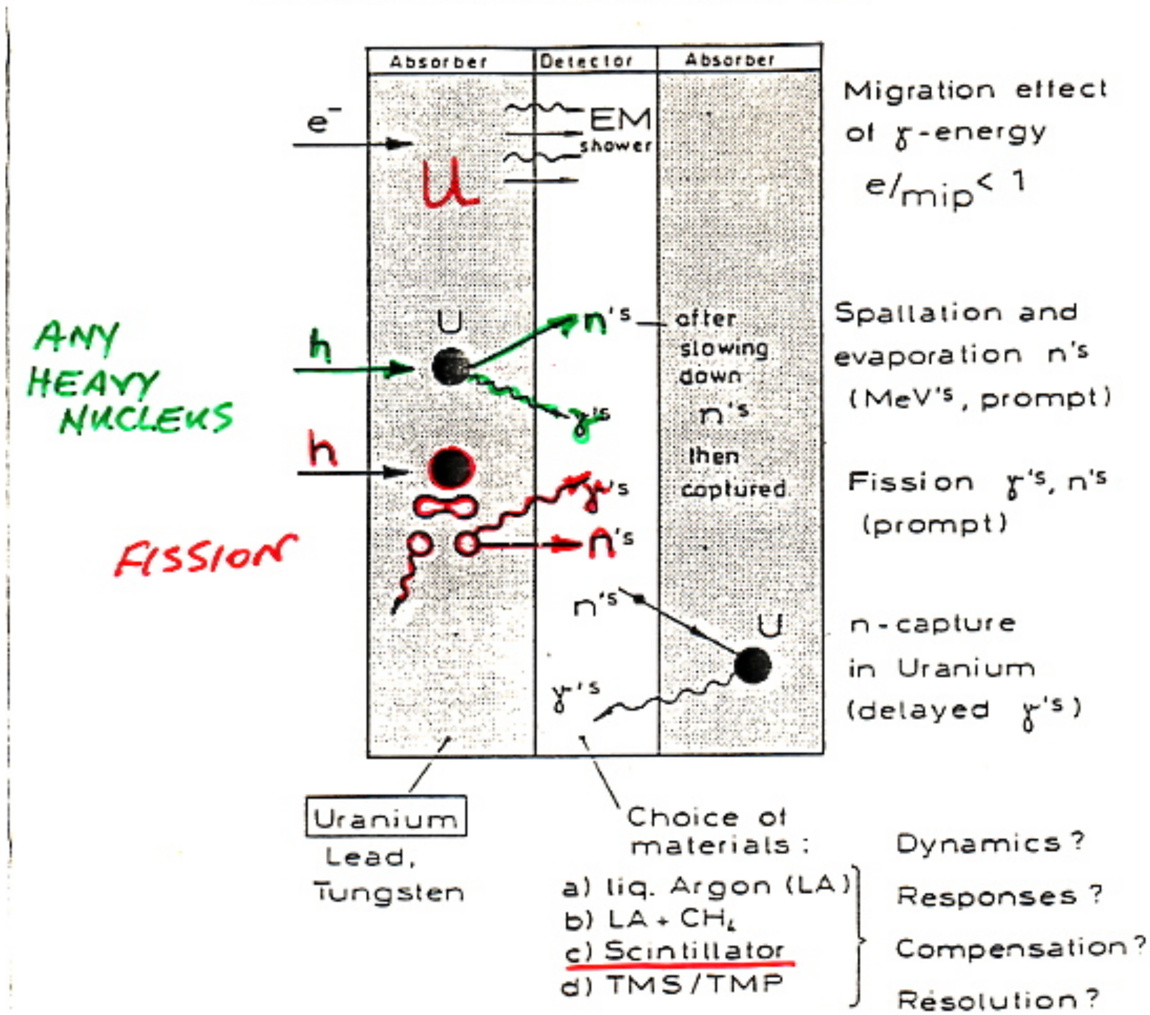

- BOOST HADRONIC RESPONSE

URANIUM → γ, n

Weighting to Correct for e/h

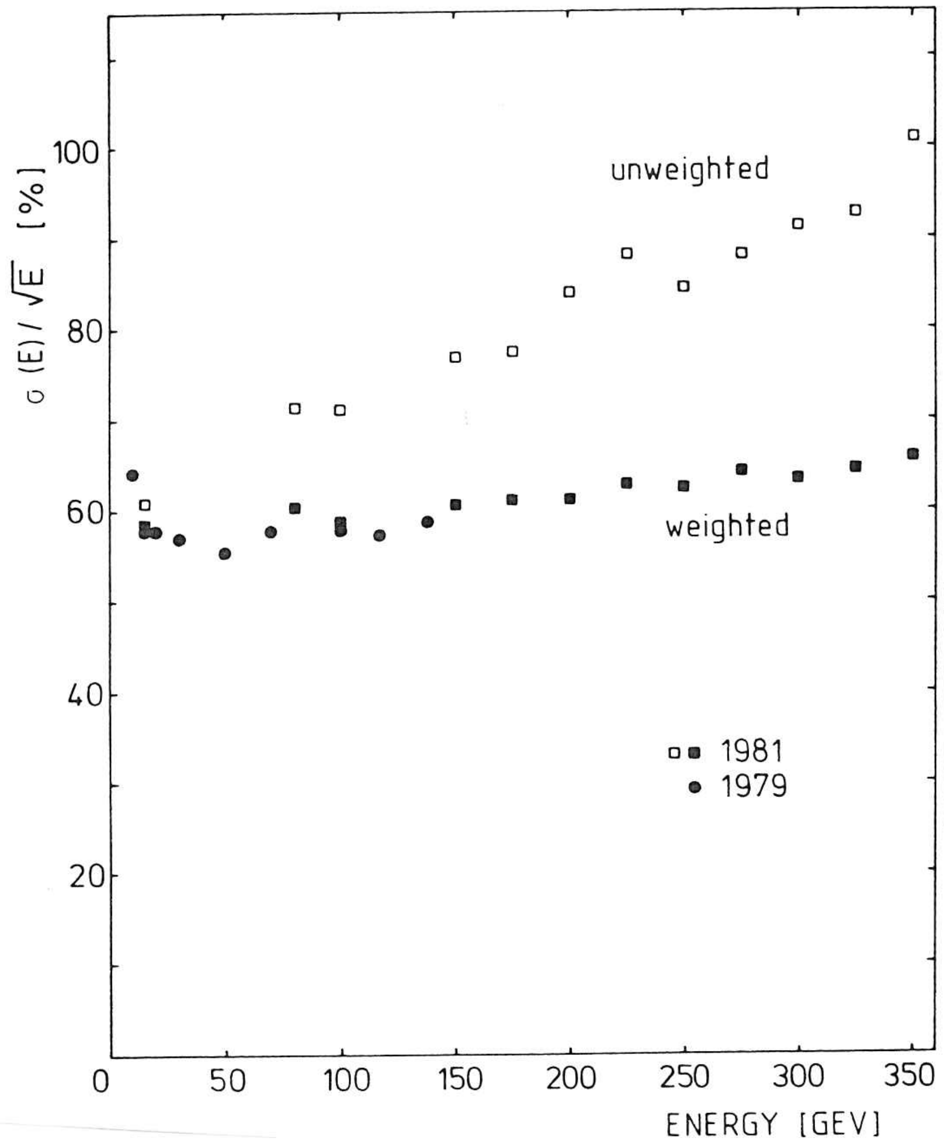

Energy resolution does not improve

$$\frac{1}{\sqrt{E}} \qquad \frac{e}{h} \neq 1$$

$$\frac{e}{h} > 1$$

Weight down EM part of shower

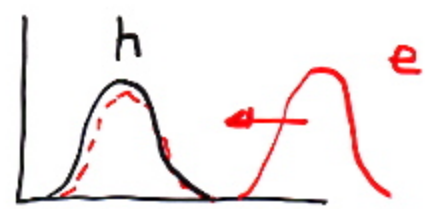

$$E_k' = E_k\left(1 - c \cdot E_k\right)$$

tune

Jet Energy Resolution

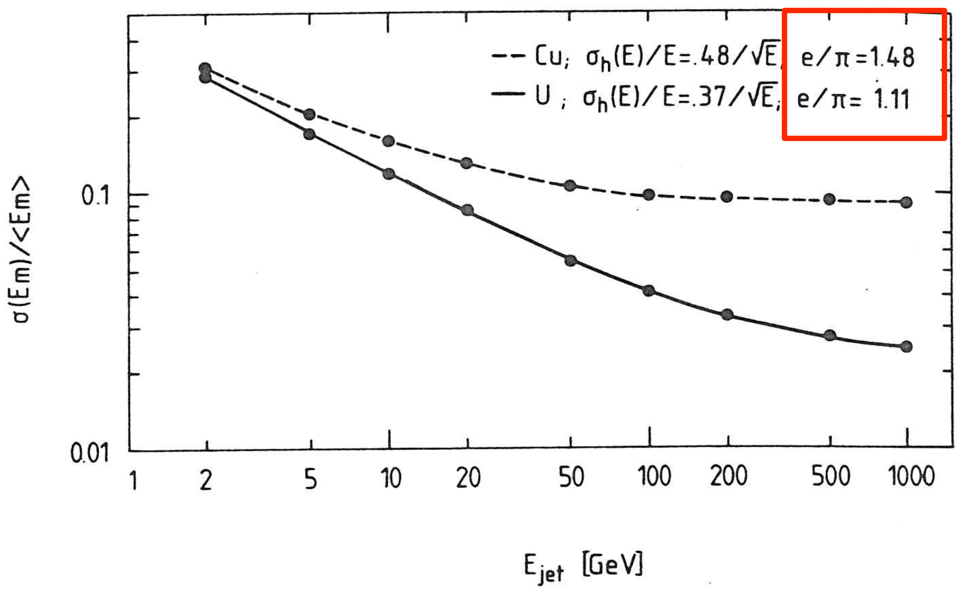

Fluctuations between EM and Hadronic component in jets will degrade the energy resolution for jets

Jet-jet Mass Resolution

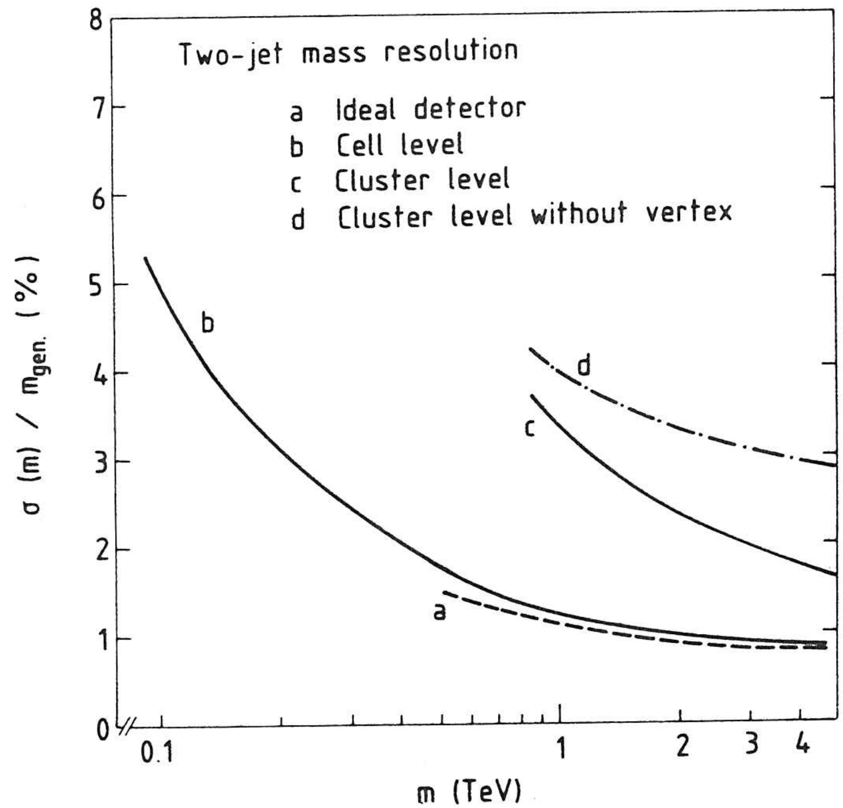

Effects other than e/h dominate the 2-jet mass resoluton

Jet-Jet Mass Resolutions

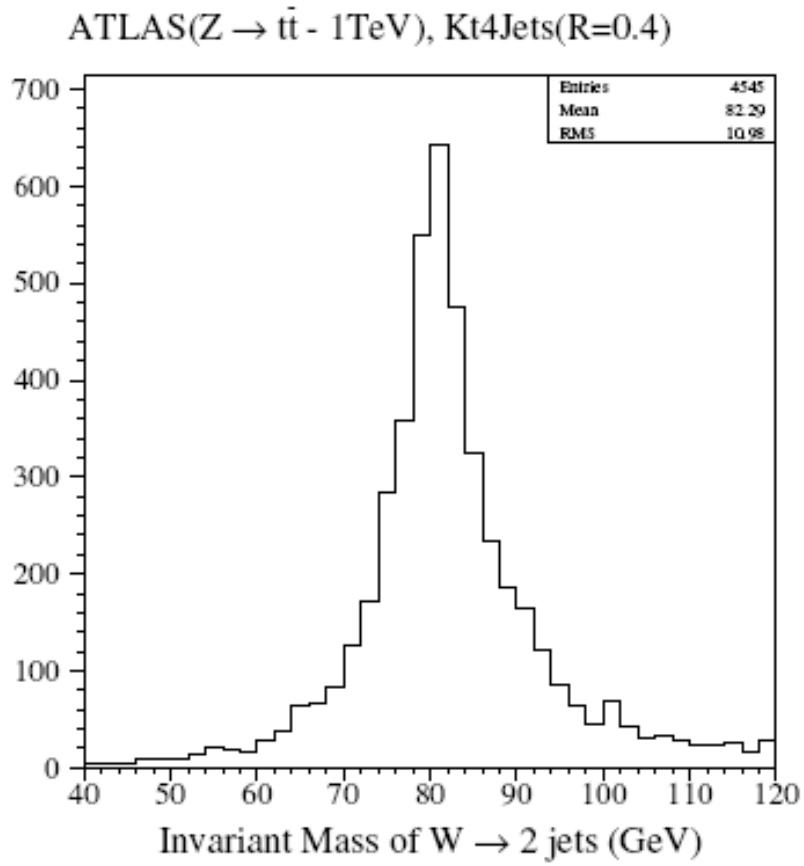

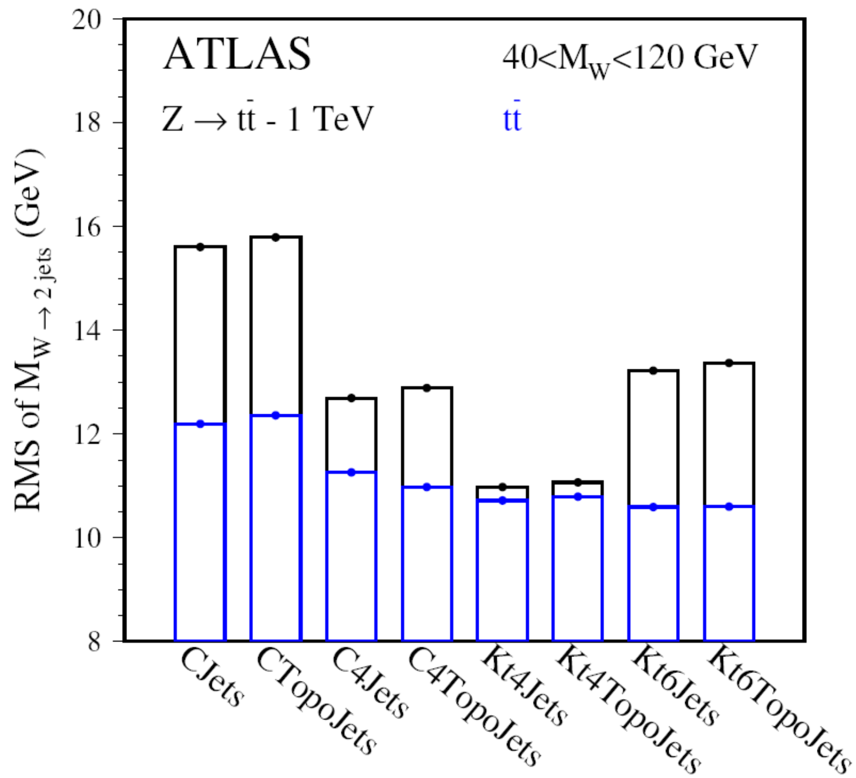

Conceptual Readout Schemes

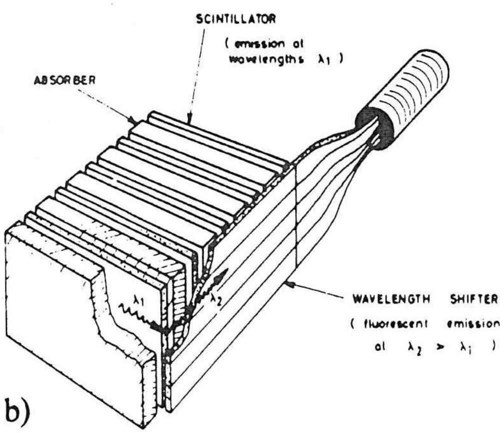

b)

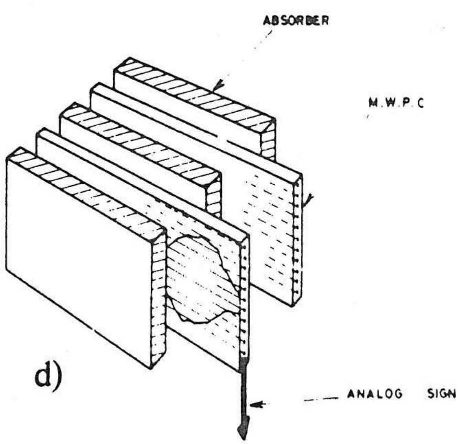

d)

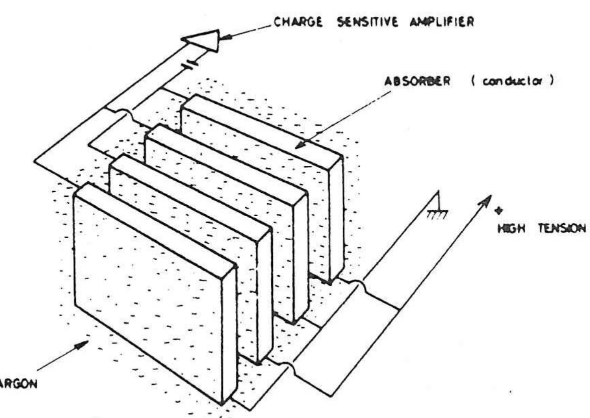

c)

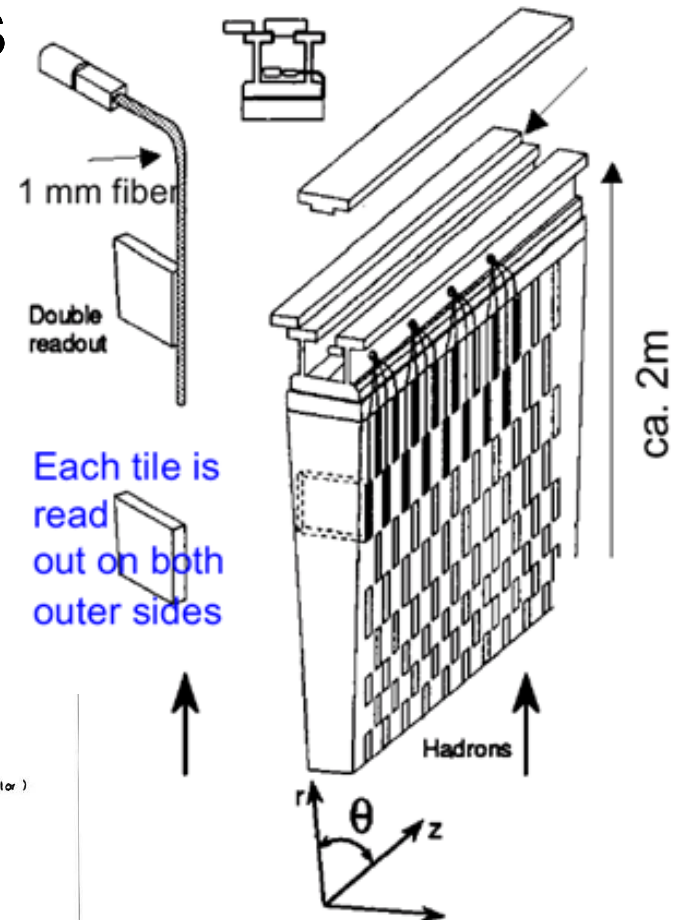

ZEUS Forward Calorimeter

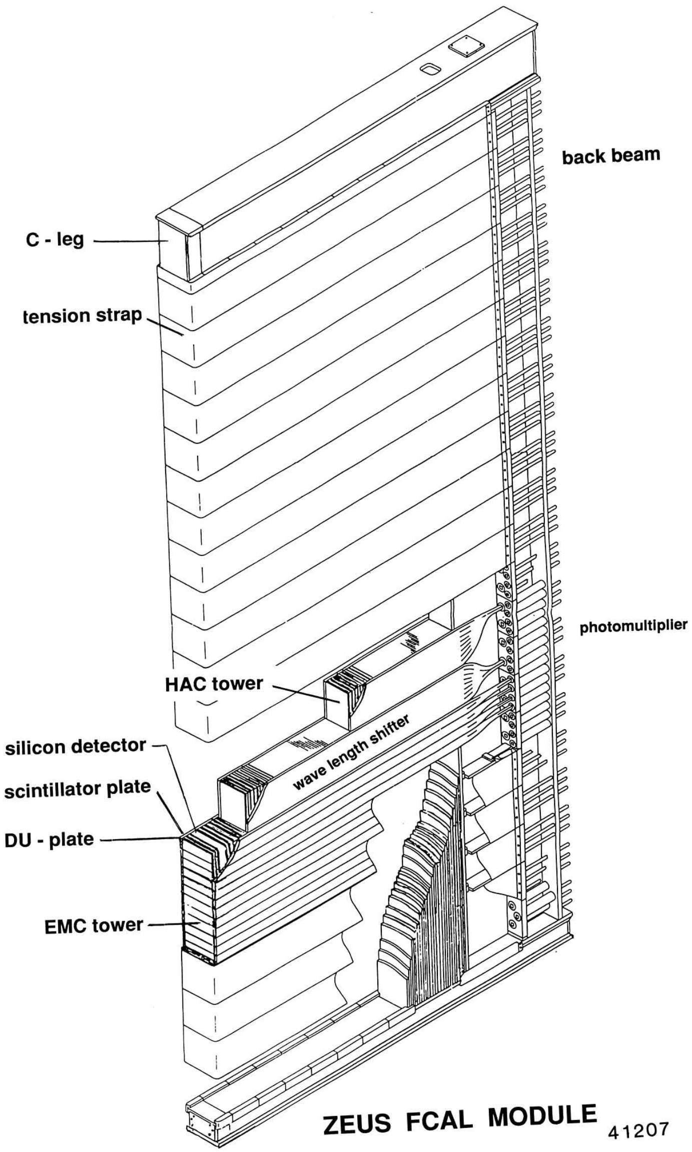

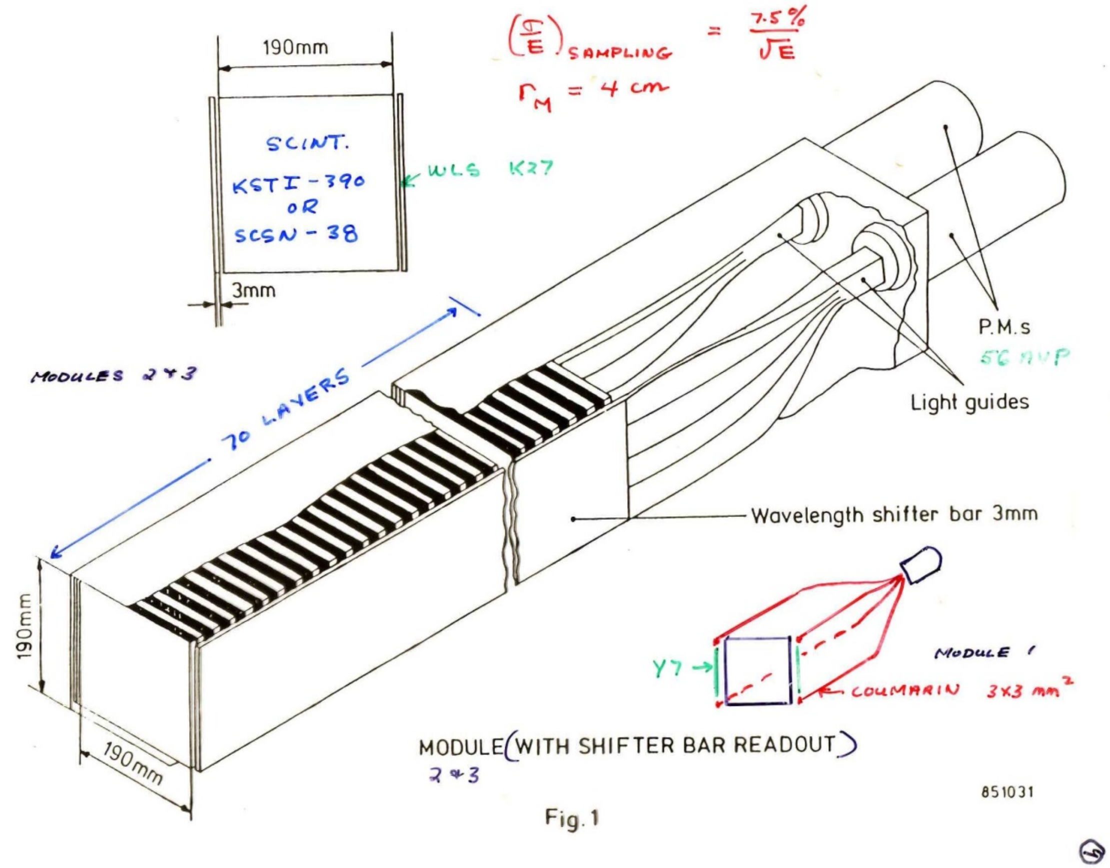

$\left(\frac{\sigma}{E}\right)_{SAMPLING} = \frac{7.5\%}{\sqrt{E}}$

$r_M = 4$ cm

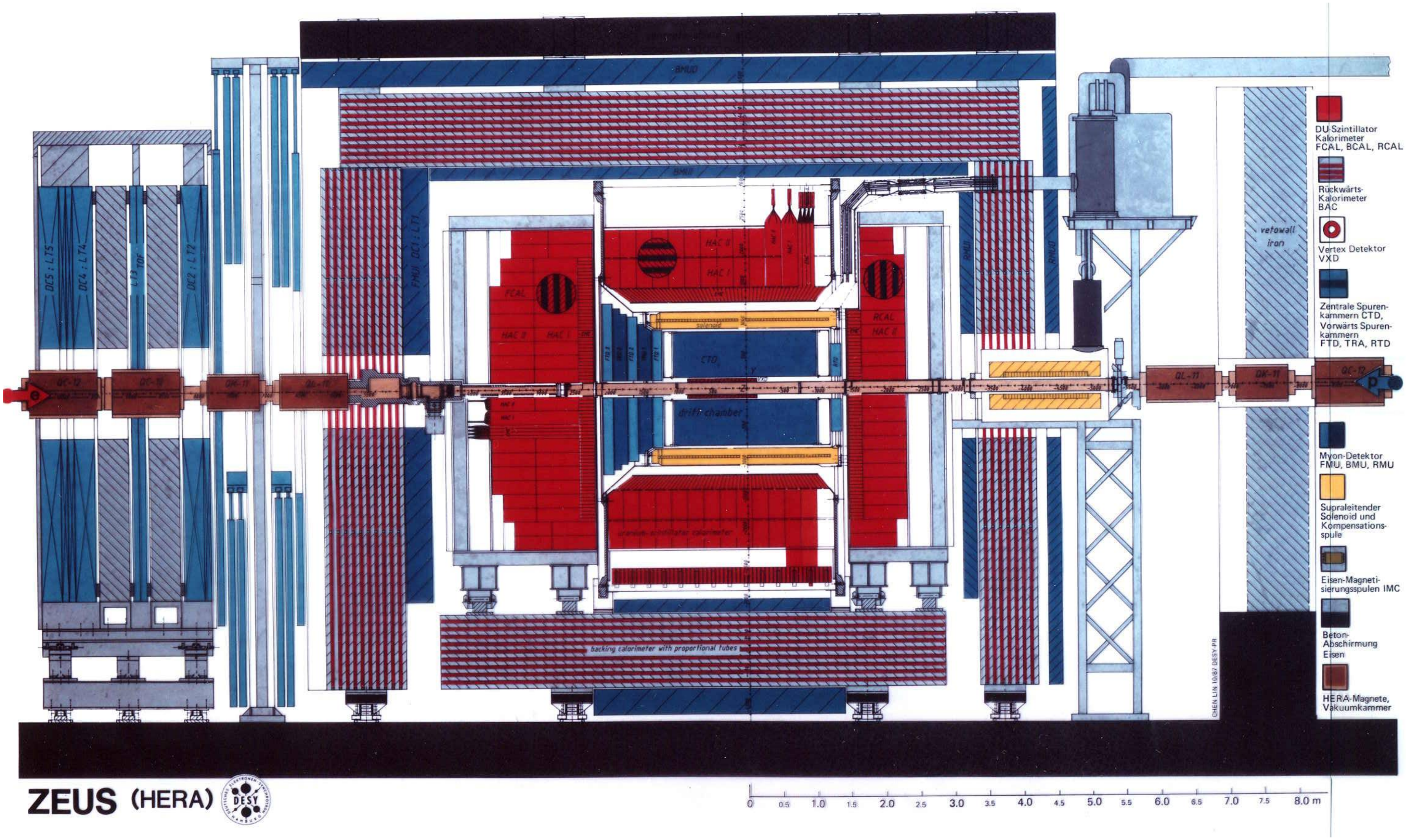
DU-Szintillator Kalorimeter FCAL, BCAL, RCAL
Rückwärts-Kalorimeter BAC
Vertex Detektor VXD
Zentrale Spurenkammern CTD, Vorwärts Spurenkammern FTD, TRA, RTD
Myon-Detektor FMU, BMU, RMU
Supraleitender Solenoid und Kompensationsspule
Eisen-Magnetisierungsspulen IMC
Beton-Abschirmung Eisen
HERA-Magnete, Vakuumkammer
FCAL
RCAL
CTD
drift chamber
backing calorimeter with proportional tubes
vetowall iron
e
p
ZEUS (HERA)
0 0.5 1.0 1.5 2.0 2.5 3.0 3.5 4.0 4.5 5.0 5.5 6.0 6.5 7.0 7.5 8.0 m

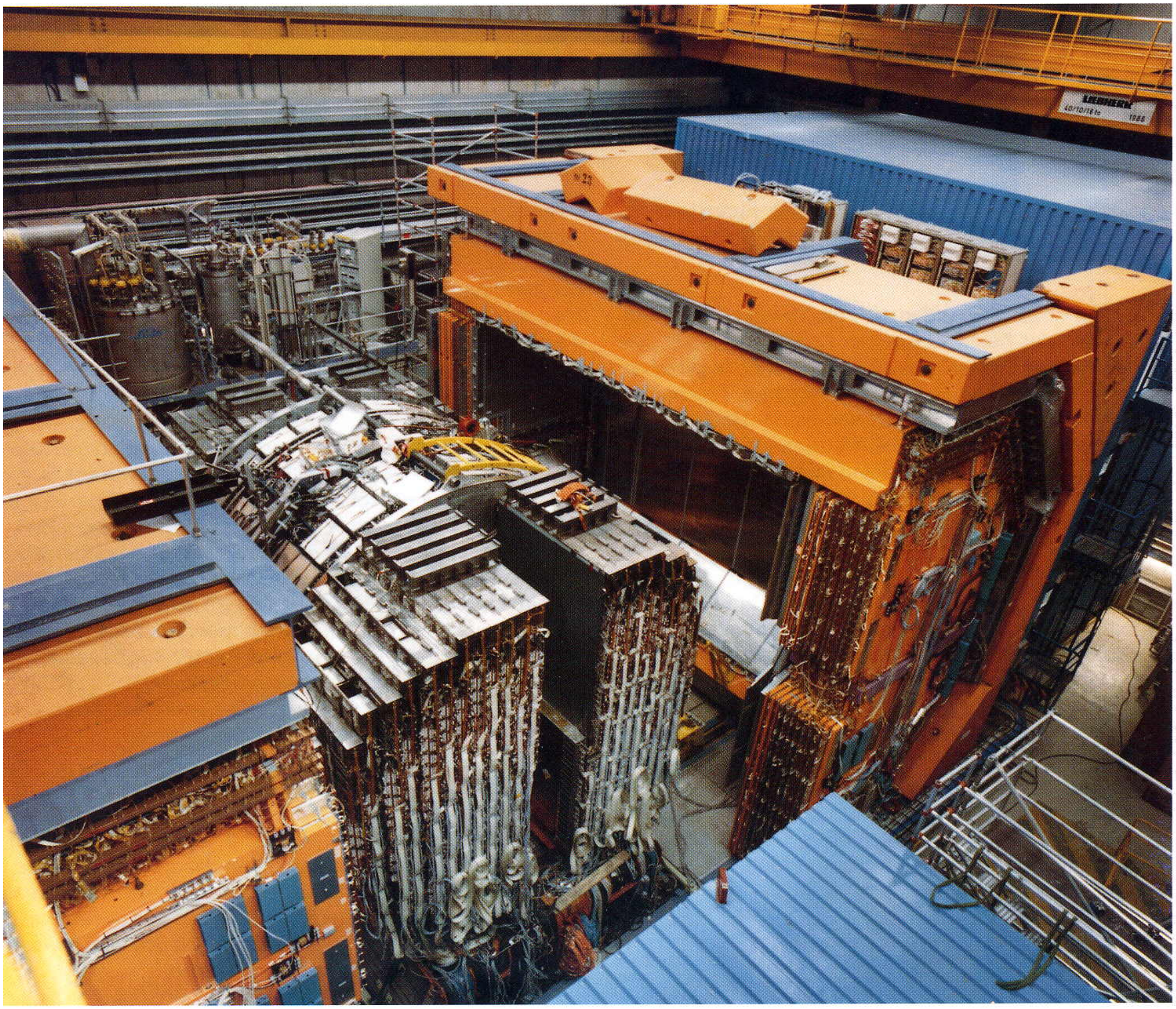

oint

LAr Calorimetry

- Five different detector technologies
- Calorimetry coverage to

$|\eta|$; 5

SM Higgs Discovery Potential

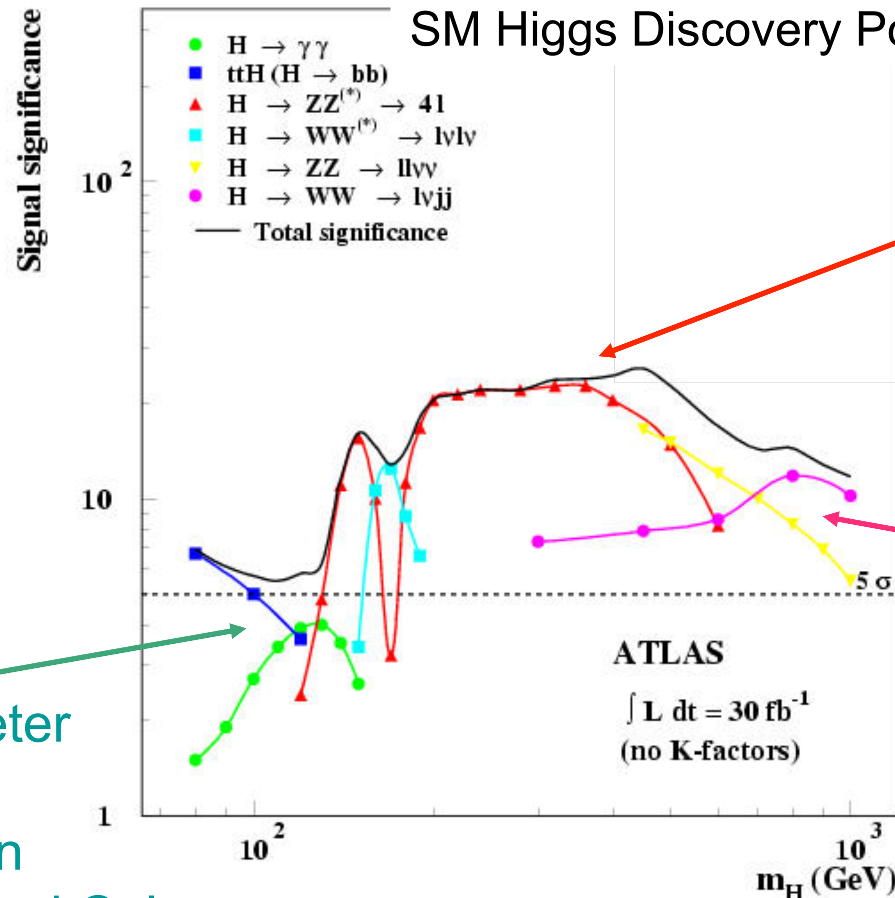

$H \rightarrow 4l$

EM Calorimeter

$H \rightarrow ZZ$ & $H \rightarrow WW$

Hadronic & Forward Calorimeters

$H \rightarrow \gamma\gamma$

EM Calorimeter

WW Fusion
Tag jets in Forward Cal

LAr Calorimeter Technology Overview

Design Goals ➡ Technology

- **EM Calorimeters** ($0 \le |\eta| \le 3.2$) and Presampler ($0 \le |\eta| \le 1.8$)

$$\frac{\sigma}{E} \le \frac{10\%}{\sqrt{E(\mathrm{GeV})}} \oplus 0.7\% \oplus \frac{0.27}{E(\mathrm{GeV})} \qquad \sigma_\theta \le \frac{40\ \mathrm{mrad}}{\sqrt{E(\mathrm{GeV})}} \qquad \sigma_{\vec{r}} \le \frac{8\ \mathrm{mm}}{\sqrt{E(\mathrm{GeV})}}$$

➡ Lead/Copper-Kapton/Liquid Argon *Accordion* Structure

- **Hadronic Endcap** ($1.5 \le |\eta| \le 3.2$)

$$\frac{50\%}{\sqrt{E(\mathrm{GeV})}} \oplus 3\% \le \frac{\sigma}{E}(\mathrm{jets}) \le \frac{100\%}{\sqrt{E(\mathrm{GeV})}} \oplus 10\%$$

➡ Copper/Copper-Kapton/Liquid Argon *Plate* Structure

- **Forward Calorimeter** ($3 \le |\eta| \le 5$)

$$\frac{\sigma}{E}(\mathrm{jets}) \le \frac{100\%}{\sqrt{E(\mathrm{GeV})}} \oplus 10\%$$

➡ Tungsten/Copper/Liquid Argon *Paraxial Rod* Structure

LAr and Tile Calorimeters

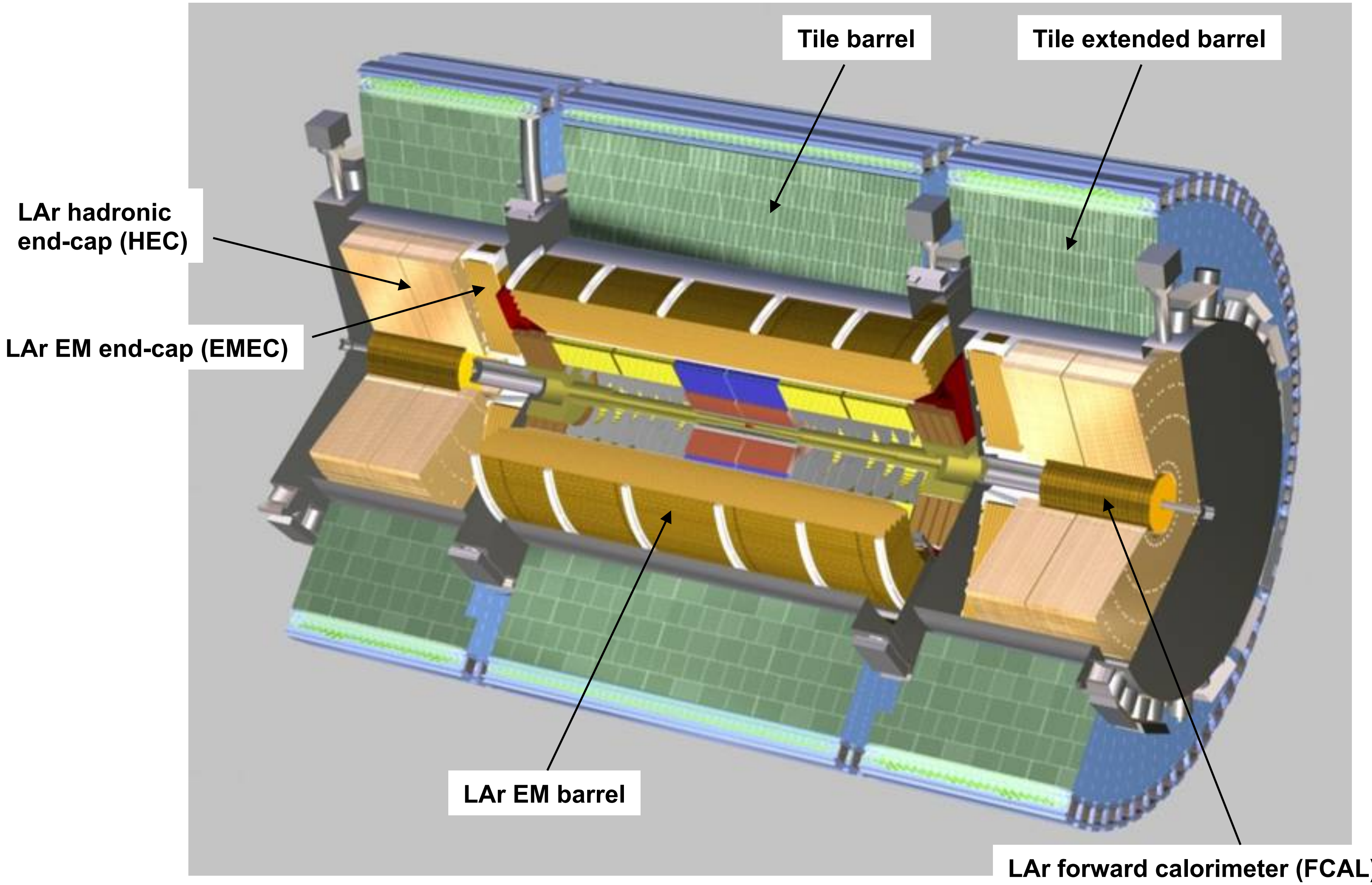

Electromagnetic Barrel

$0 < \eta < 1.4$

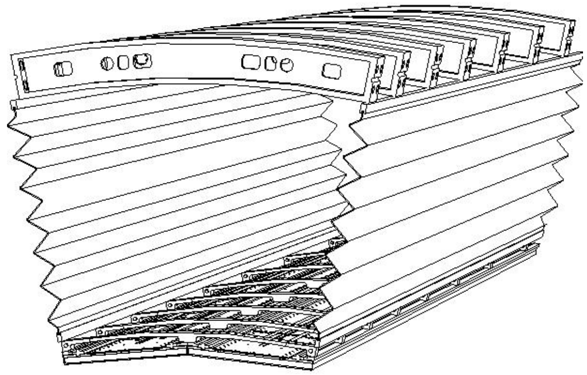

Barrel Module Schematic
with presampler

- 64 gaps /module
- 2.1 mm gap
- 2x3100 mm long

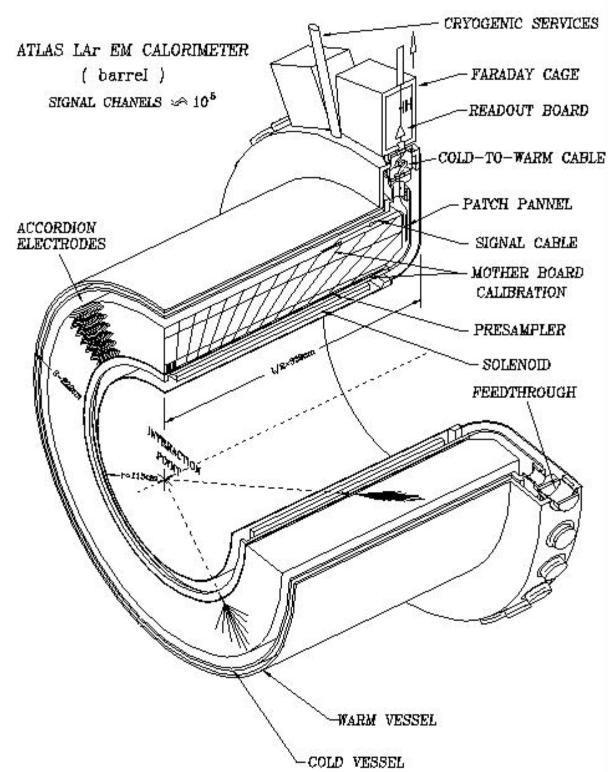

Half Barrel Assembly

- 2x16 modules
- I.R/O.R 1470/2000 mm
- 22 - 33 X_0
- 3 longitudinal samples
- $\Delta\eta \times \Delta\varphi \quad 0.025 \times 0.025$
- presampler $|\eta| < 1.8$

Electromagnetic Endcap

$$1.4 < \eta < 3.2$$

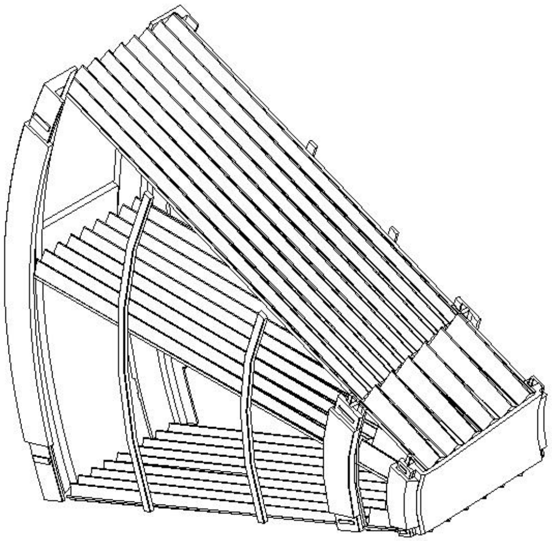

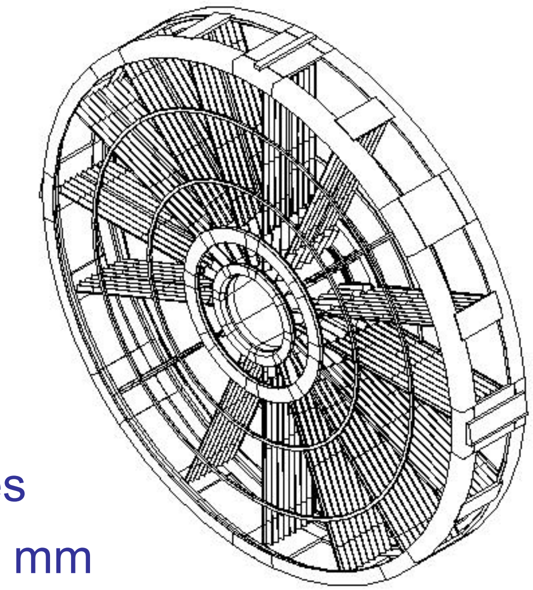

- 2x8 modules
- Diam. 4000 mm
- 22 - 37 X_0
- 3 longitudinal samples
- $\Delta\eta\times\Delta\varphi \quad 0.025\times0.025$
  $|\eta| > 2.5 \rightarrow 0.1\times0.1$
- Front sampling of 6 X_0
  for $|\eta| < 2.5$, - strips.

- 96 gaps /module outer wheel
  32 gaps/module inner wheel
- 2.8 - 0.9 mm gap outer
  3.1-1.8 mm inner

Accordion Structure

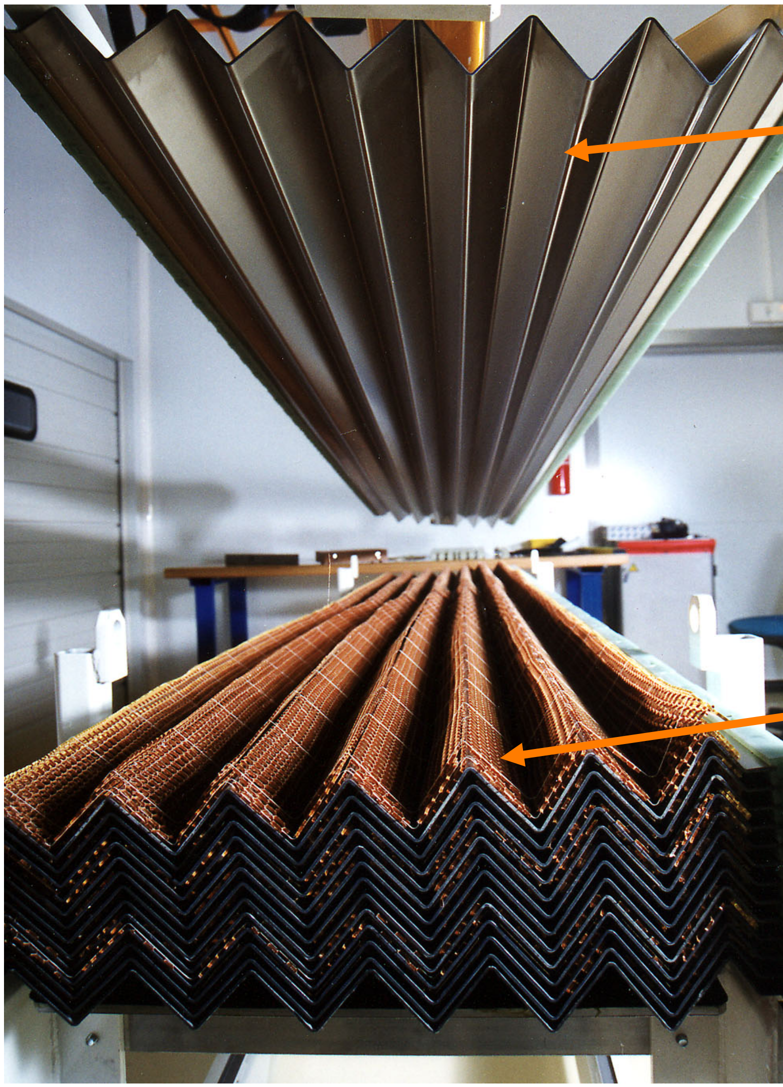

Pb Absorber

- Honeycomb spacer

&

- Cu/Kapton electrode

Prototype of EM endcap

Detail of Kaptons

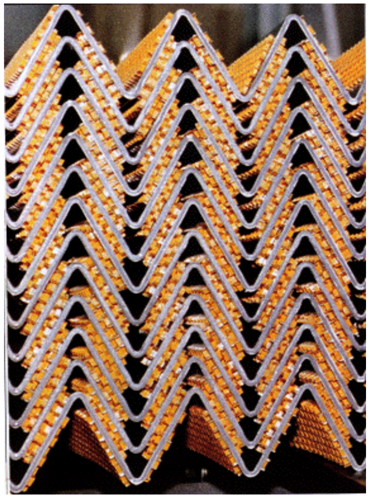

ATLAS FCAL

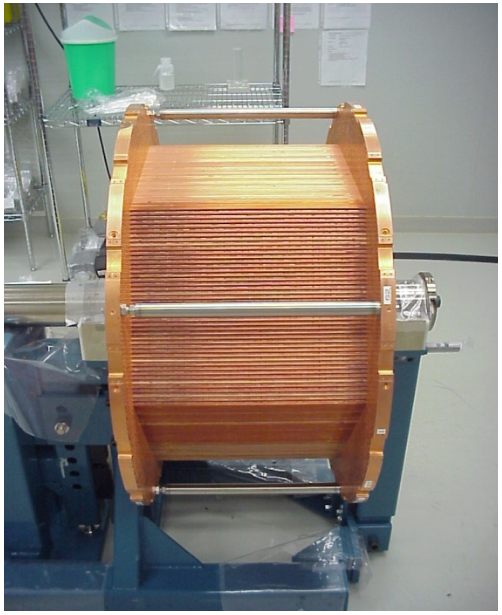

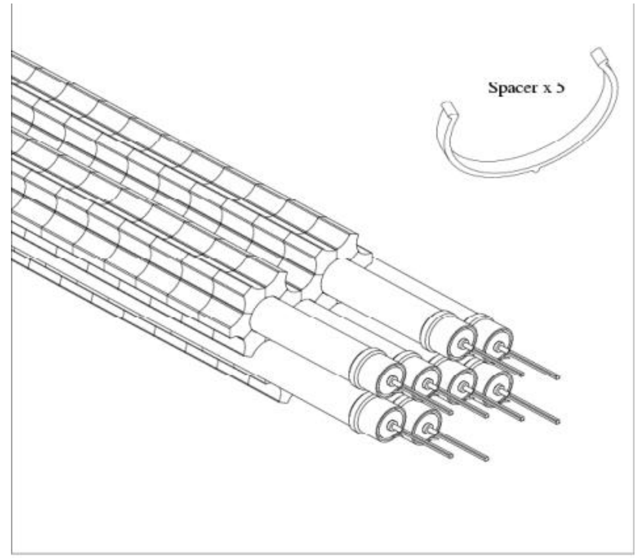

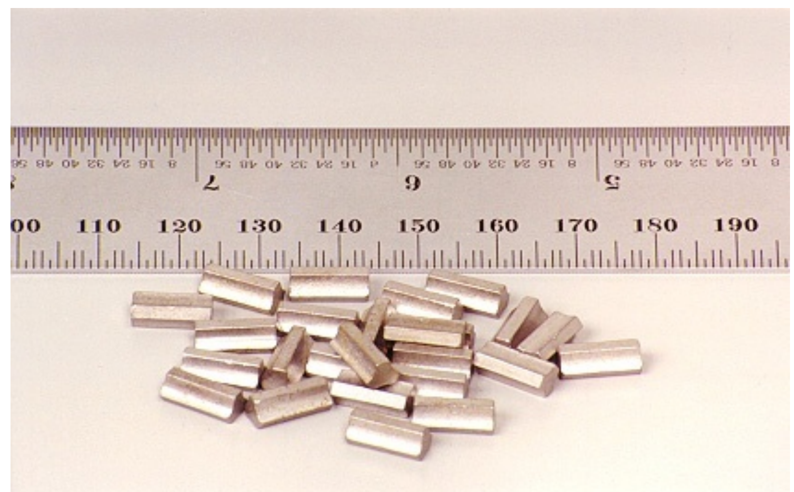

Pictures of assembly process

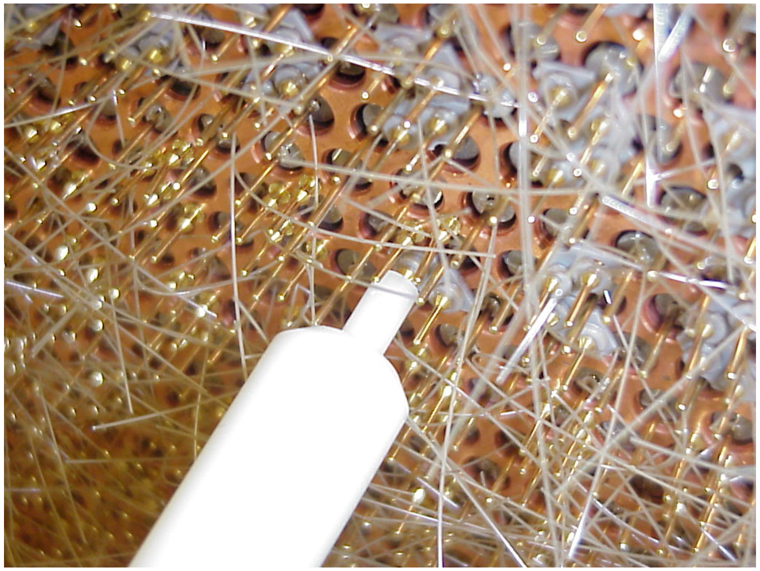
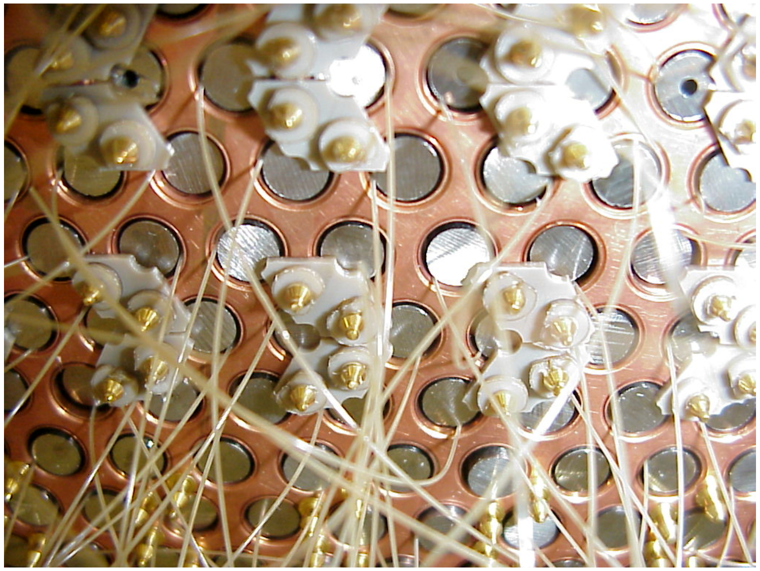
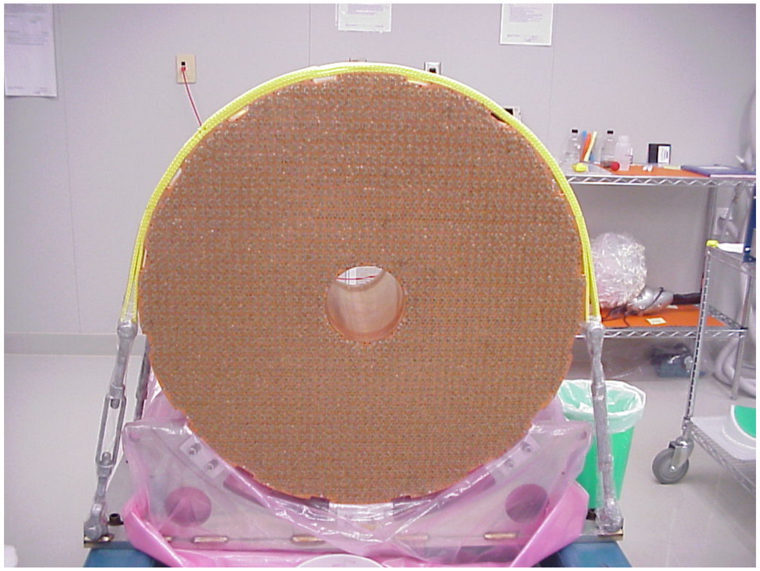


LAr Forward Calorimeters

• FCAL C assembly into tube – Fall 2003

Liquid Argon Gap

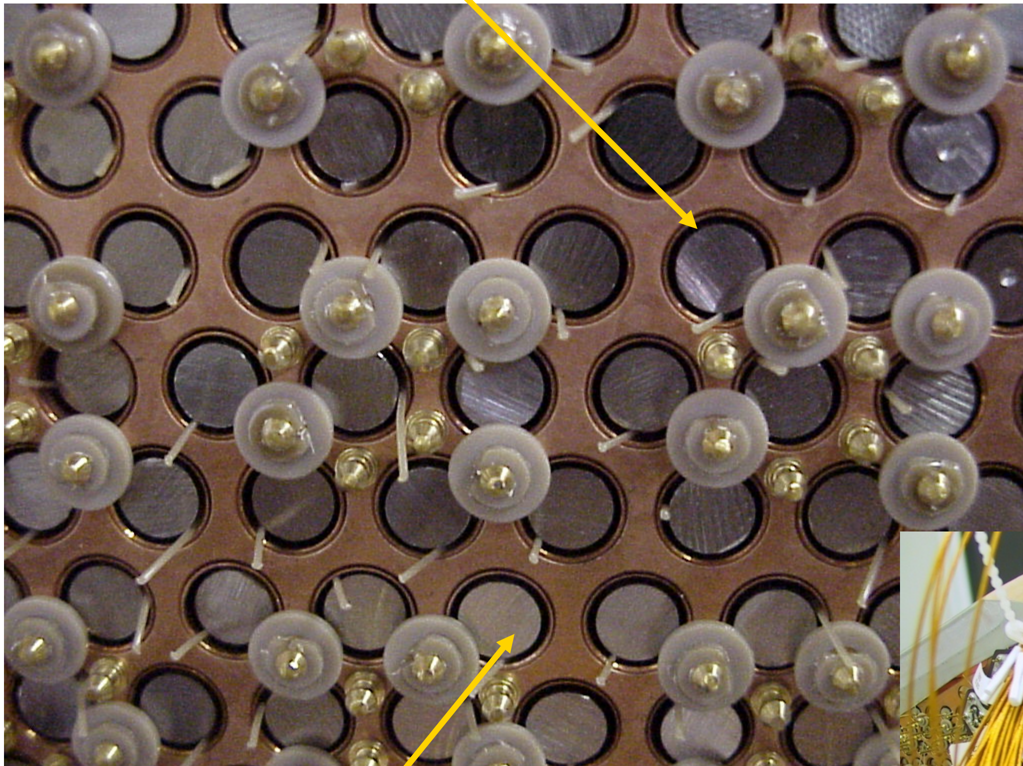

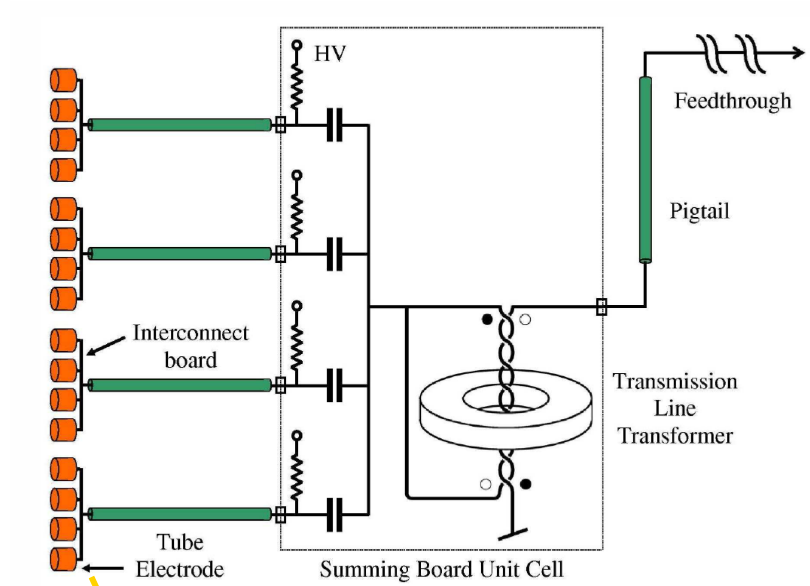

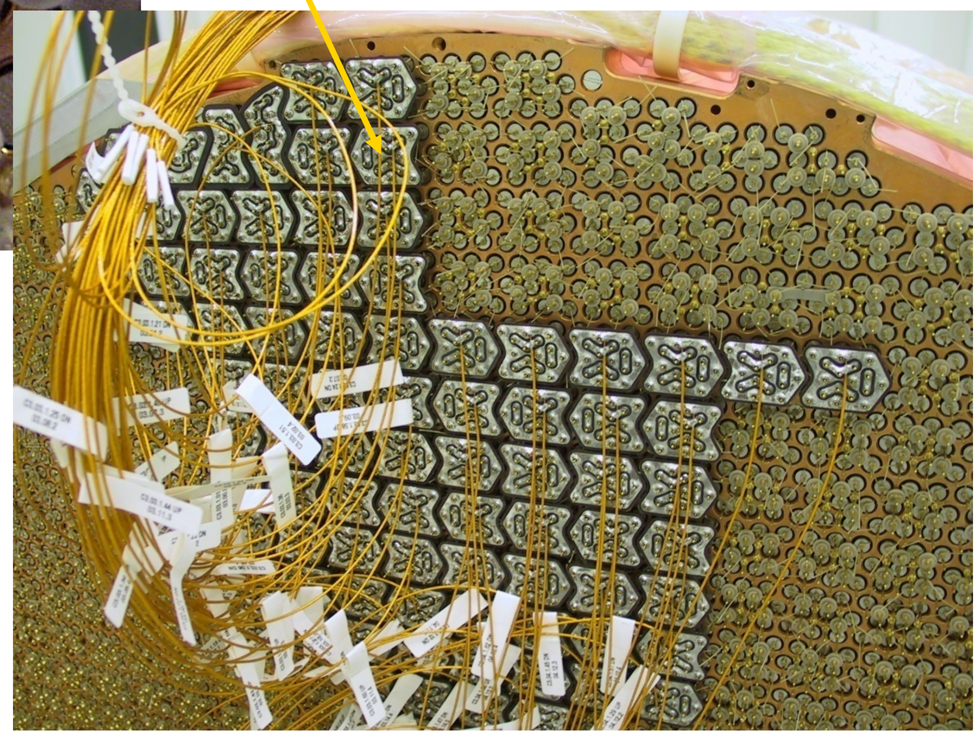

Tungsten Rod

ATLAS HEC Structure

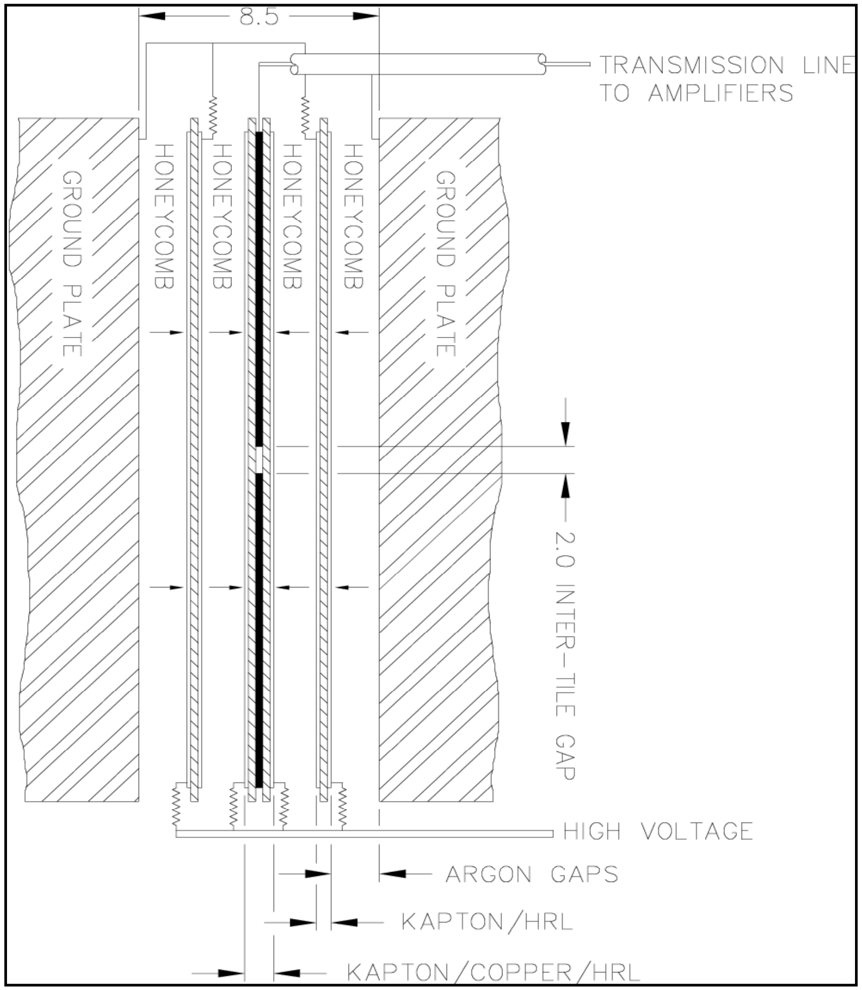

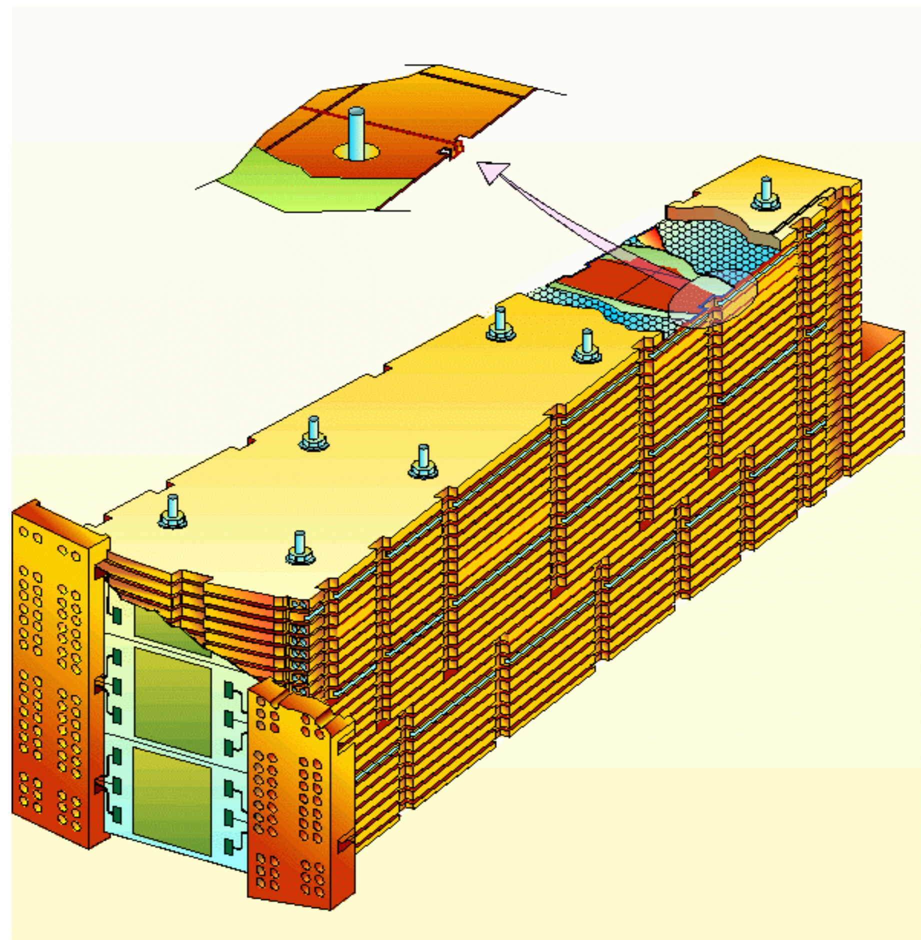

ELECTROSTATIC TRANSFORMER

- MATCHES CAL → PREAMP CAPACITANCE ← CHARGE TRANSFER TIME
- REDUCES EFFECTIVE CAPACITANCE ← NOISE

- Transformer matching
- Does not work in magnetic field. Long readout cables slow down signal
- Large capacitance, large noise

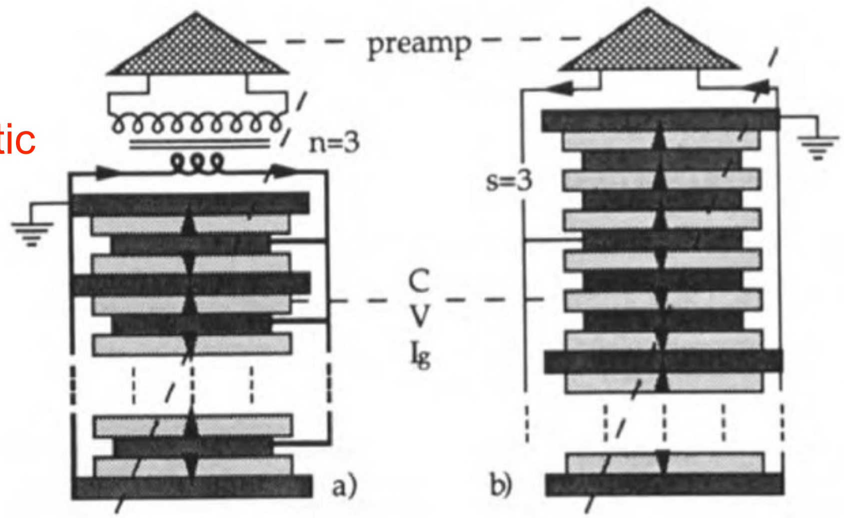

Fig. 1. Schematic representation of capacitance matching for a hadronic tower. High voltage connections are not shown. I_g is the ionization current in the gth gap. V and C are the dc voltage and capacitance per gap, respectively. The arrows show the directions of current flow. In (a) all N gaps are connected in parallel; matching is achieved with a ferrite-core transformer with turns ratio $n=3$. (b) shows an electrostatic transformer with P parallel subtowers of $S=3$ gaps in series ($N=SP$).

- EST
- Works in magnetic field
- Low capacitance

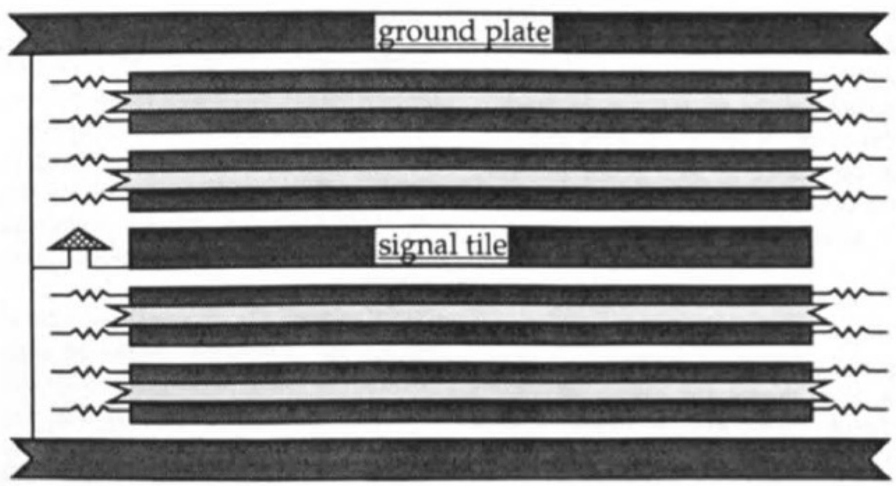

Fig. 2. Schematic view of two subsections of the tower with an electrostatic transformer of ratio $S=3$. The absorbing signal tile is at dc ground. High voltages, decoupled by large resistances, are supplied to the half tiles, which are separated by thin insulating layers.

Hadronic Endcap Calorimeter (HEC)

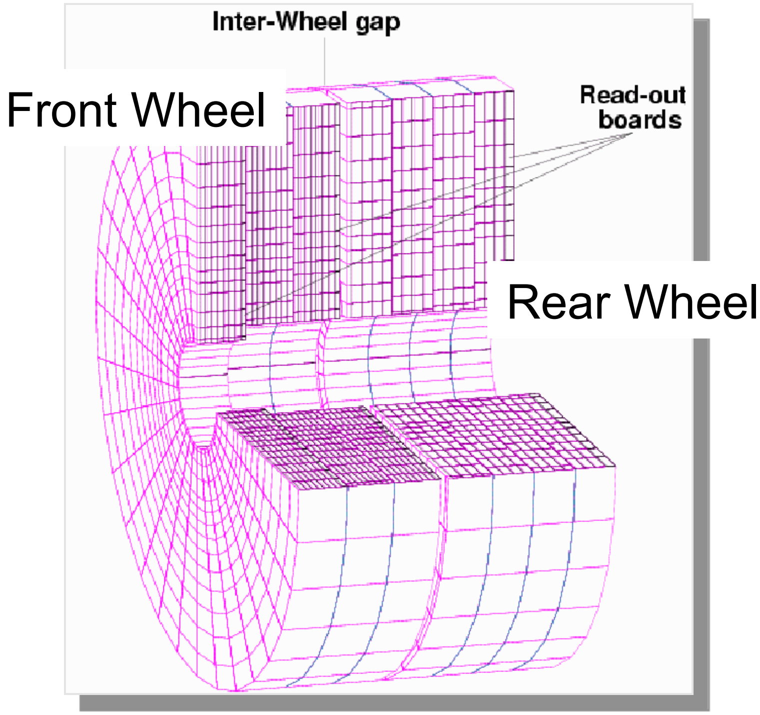

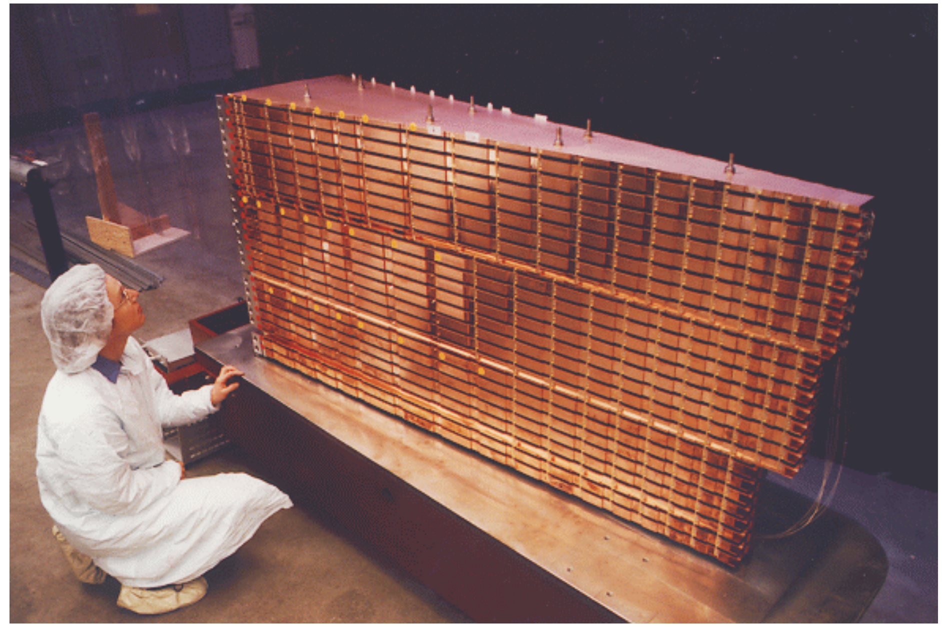

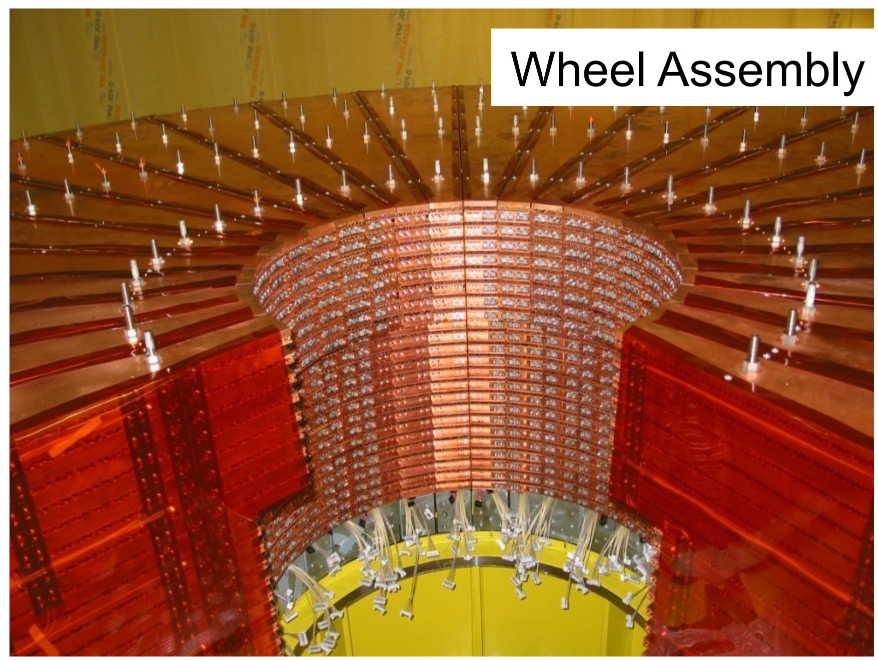

Composed of 2 wheels per end
Front wheel: 67 t 25 mm Cu plates
Back wheel: 90 t   50 mm Cu plates

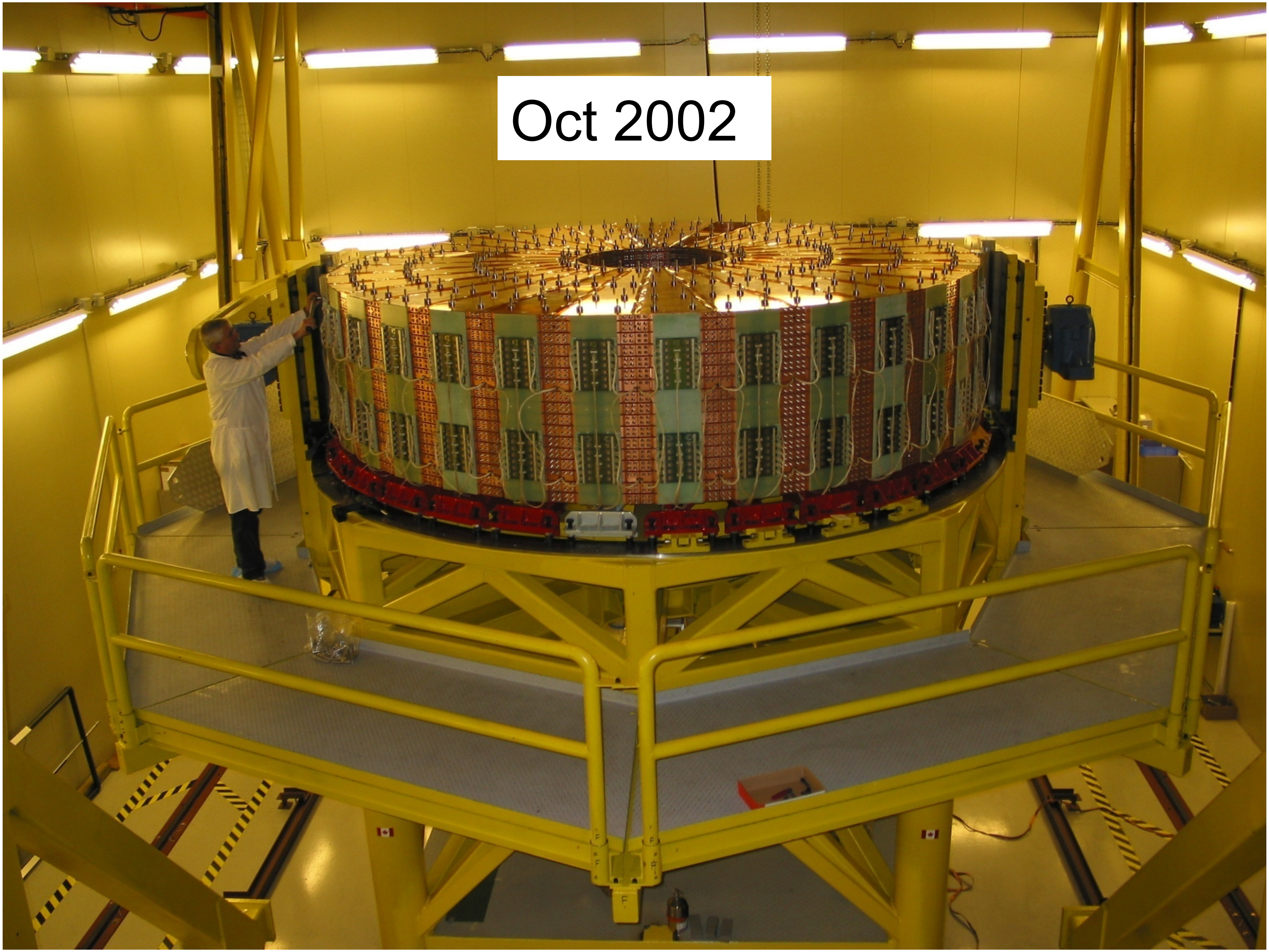
Oct 2002

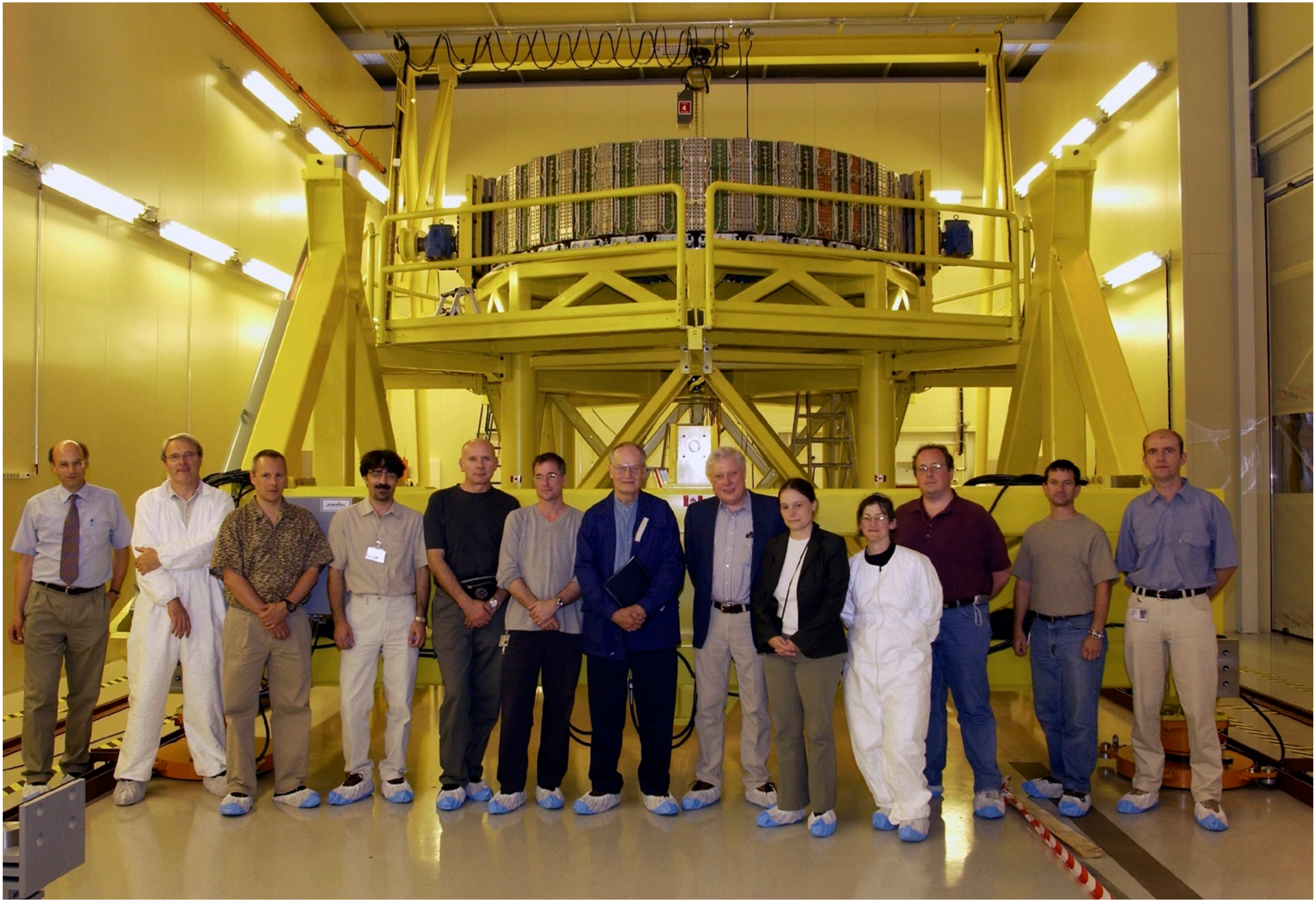

Electromagnetic Endcap

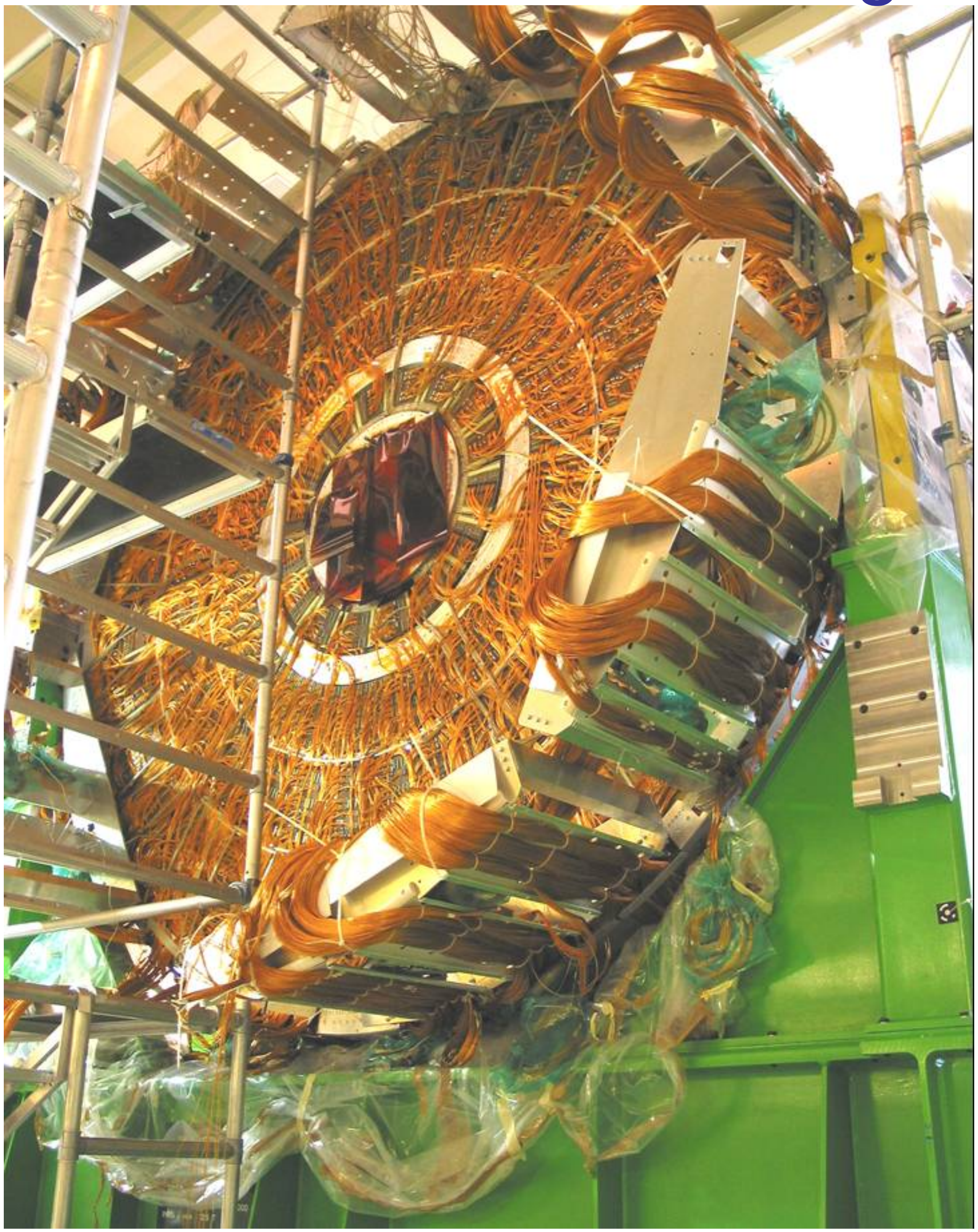

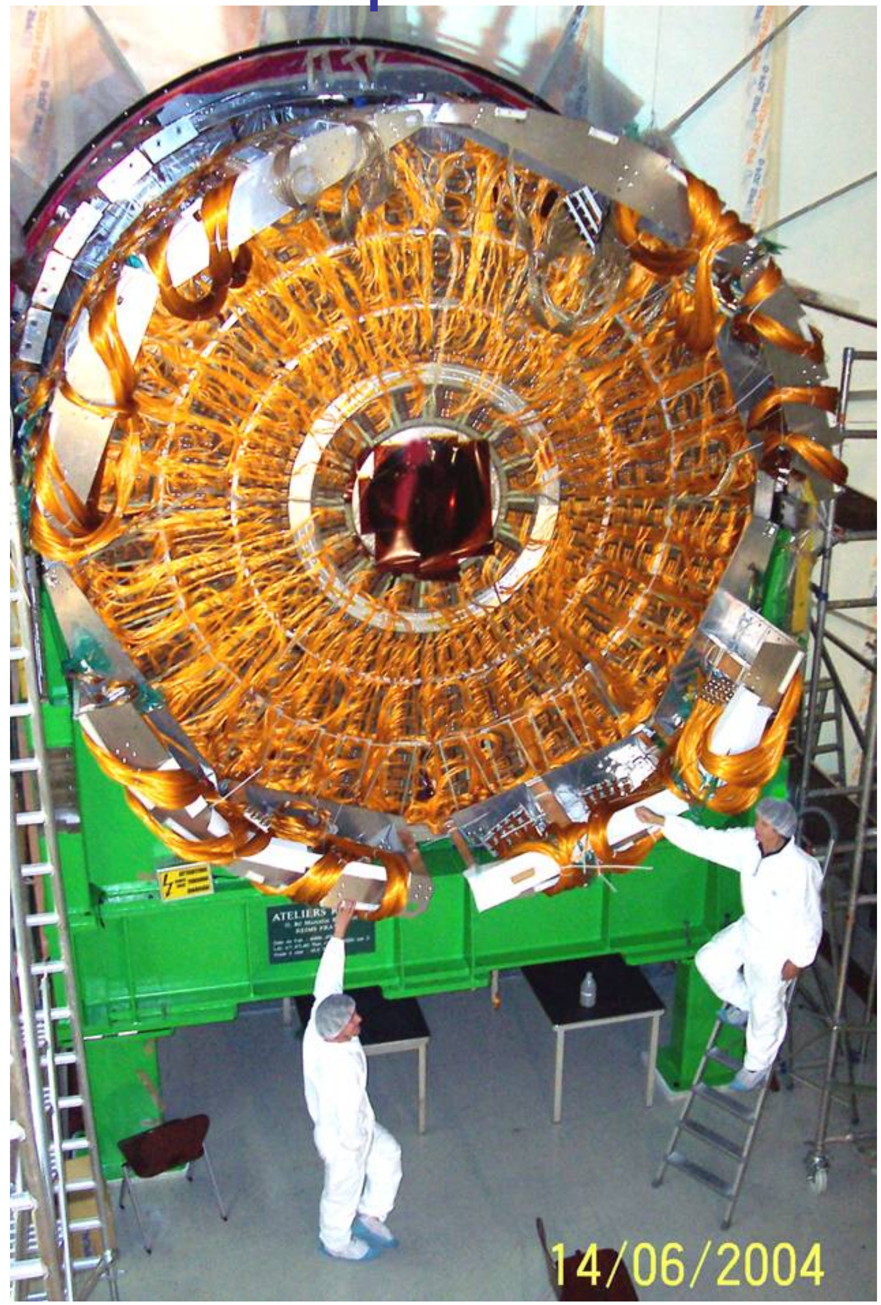

Hadronic Endcap

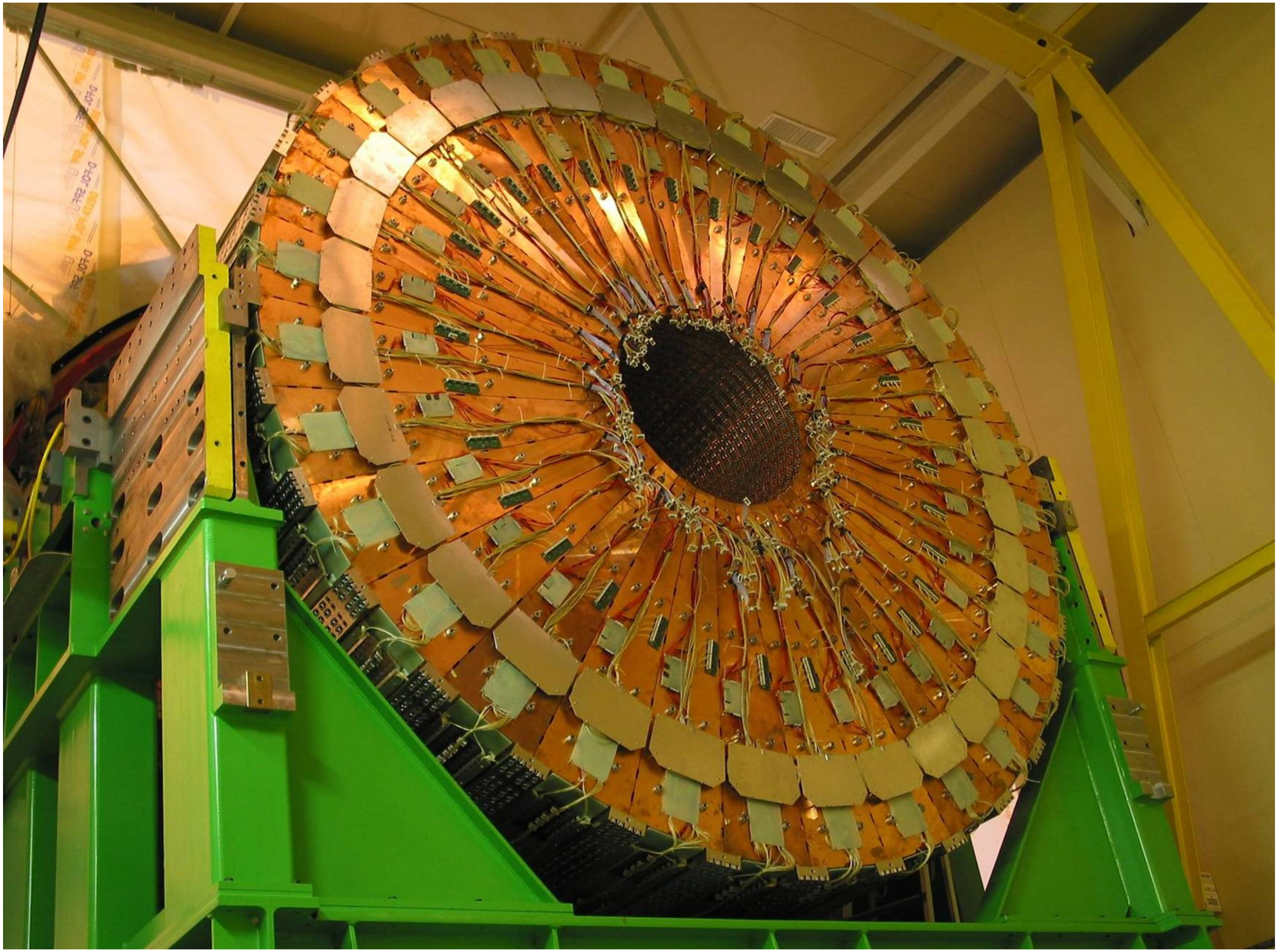

HEC – FCAL Assembly

Test Beam Single Particle Energy Resolution

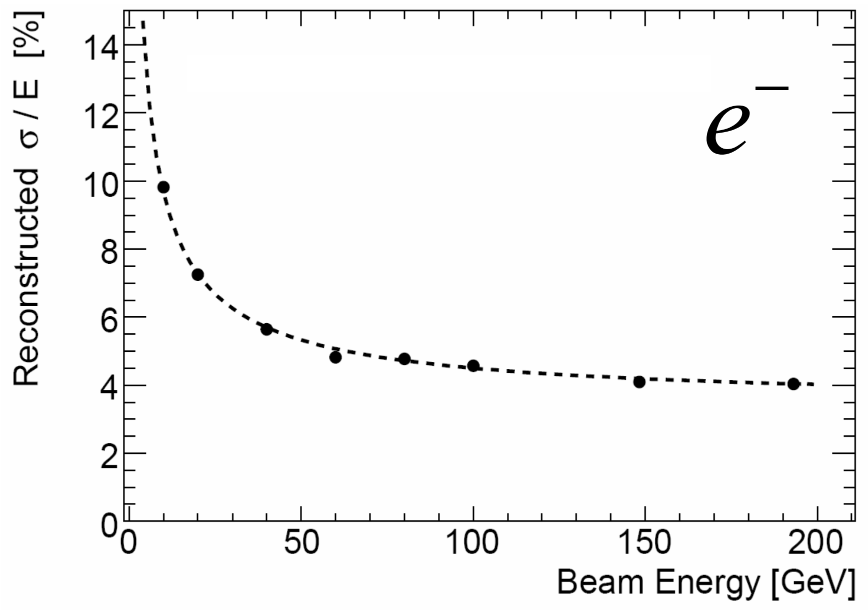

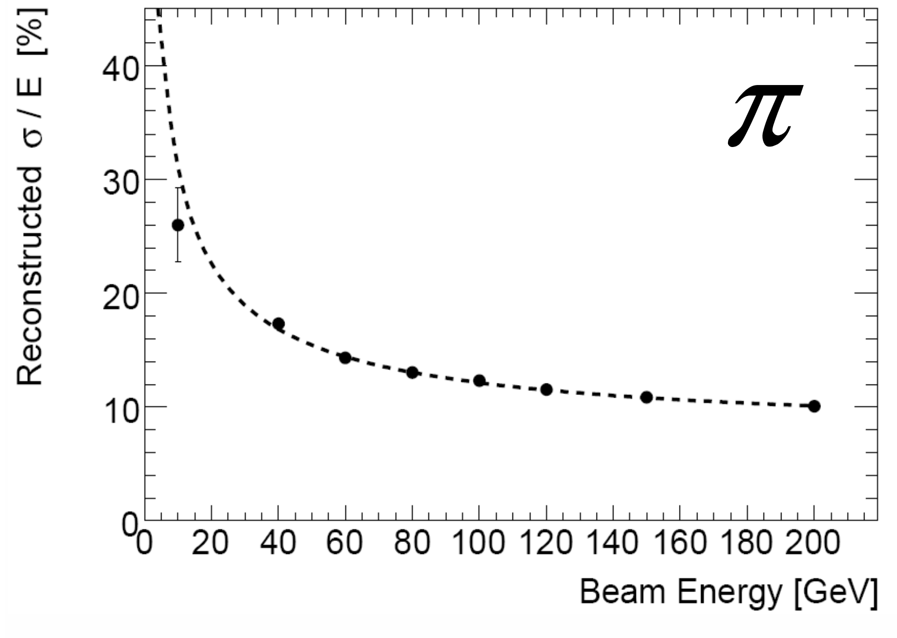

$$\frac{\sigma_E}{E} = \frac{a}{\sqrt{E}} \oplus b$$

Noise subtracted energy resolution

$$a = (28.5 \pm 1.0)\% \cdot \sqrt{GeV}$$
$$b = (3.5 \pm 0.1)\%$$

$$a = (94.2 \pm 1.6)\% \cdot \sqrt{GeV}$$
$$b = (7.5 \pm 0.4)\%$$

Noise Level in LAr Calorimeters

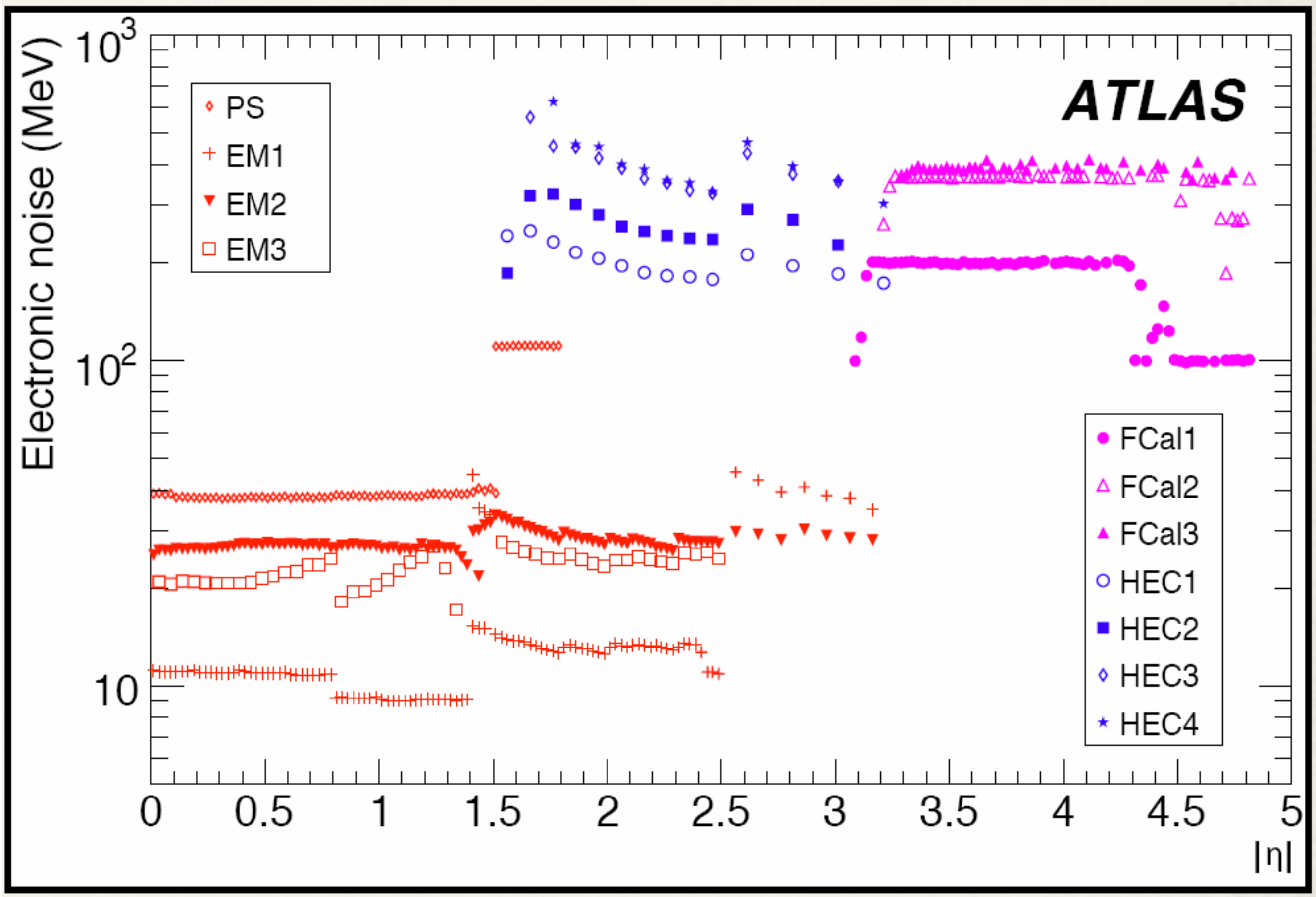

Since the FCal is in the very forward region, these noise levels are OK

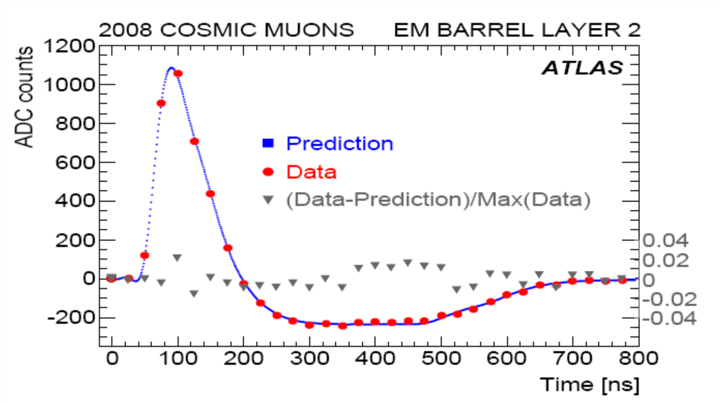

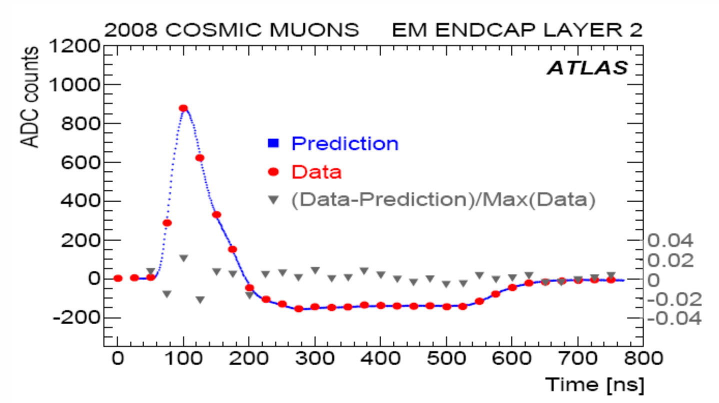

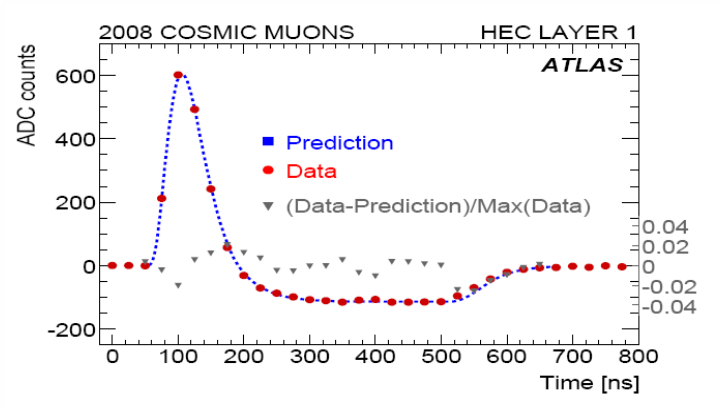

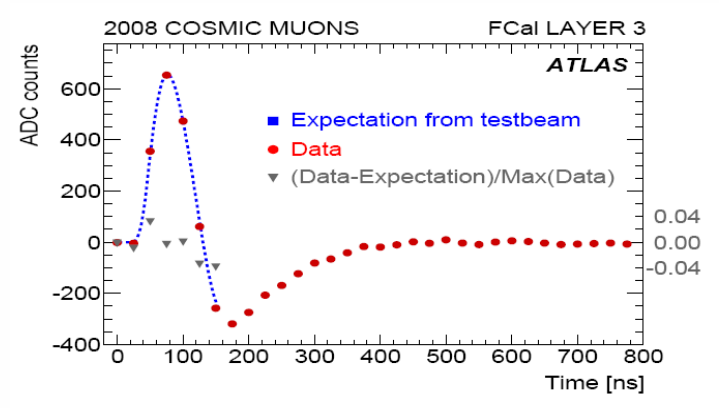

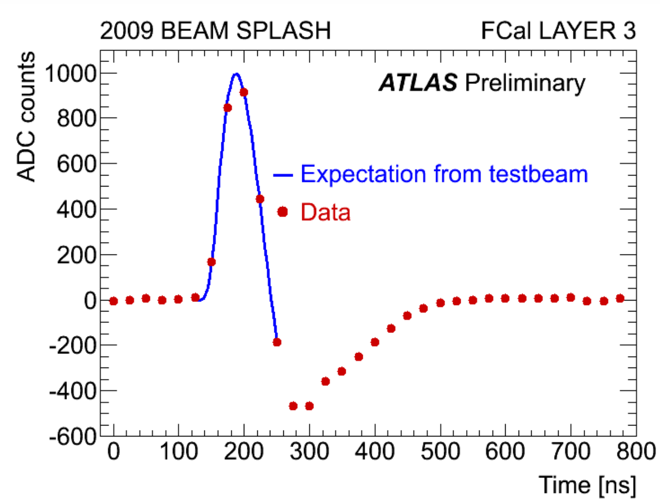

Signal Shape before startup

Lar Endcap Installed in ATLAS